applied sciences

MDPI

Systematic Review

Artificial Intelligence and Statistical Models for the Prediction of Radiotherapy Toxicity in Prostate Cancer: A Systematic Review

Antonio Piras [1,2,3,4], Rosario Corso [2,5], Viviana Benfante [3,6,*], Muhammad Ali [2,3], Riccardo Laudicella [7], Pierpaolo Alongi [6,8], Andrea D'Aviero [9,10], Davide Cusumano [11], Luca Boldrini [12,13], Giuseppe Salvaggio [14], Domenico Di Raimondo [3], Antonino Tuttolomondo [3] and Albert Comelli [2]

1 UO Radioterapia Oncologica, Villa Santa Teresa, 90011 Bagheria, Italy; apiras@fondazionerimed.com
2 RI.MED Foundation, Via bandiera 11, 90133 Palermo, Italy; rosario.corso02@unipa.it (R.C.); amuhammad@fondazionerimed.com (M.A.); acomelli@fondazionerimed.com (A.C.)
3 Department of Health Promotion, Mother and Child Care, Internal Medicine and Medical Specialties, Molecular and Clinical Medicine, University of Palermo, 90127 Palermo, Italy; domenico.diraimondo@unipa.it (D.D.R.); bruno.tuttolomondo@unipa.it (A.T.)
4 Radiation Oncology, Mater Olbia Hospital, 07026 Olbia, Italy
5 Department of Mathematics and Computer Science, University of Palermo, 90127 Palermo, Italy
6 Advanced Diagnostic Imaging—INNOVA Project, Department of Radiological Sciences, A.R.N.A.S. Civico, Di Cristina e Benfratelli Hospitals, P.zza N. Leotta 4, 90127 Palermo, Italy; pierpaolo.alongi@arnascivico.it
7 Nuclear Medicine Unit, Department of Biomedical and Dental Sciences and Morpho-Functional Imaging, Messina University, 98124 Messina, Italy; rlaudicella@unime.it
8 Nuclear Medicine Unit, A.R.N.A.S. Civico, Di Cristina e Benfratelli Hospitals, P.zza N. Leotta 4, 90127 Palermo, Italy
9 Department of Medical, Oral and Biotechnological Sciences, "G. D'Annunzio" University of Chieti, 66100 Chieti, Italy; andrea.daviero@unich.it
10 Department of Radiation Oncology, "S.S. Annunziata" Chieti Hospital, 66100 Chieti, Italy
11 Medical Physics Unit, Mater Olbia Hospital, 07026 Olbia, Italy; davide.cusumano@materolbia.com
12 Gemelli Advanced Radiotherapy Center, Fondazione Policlinico Universitario "A. Gemelli" IRCCS, 00168 Rome, Italy; luca.boldrini@policlinicogemelli.it
13 Radiomics GSTeP Core Research Facility, Fondazione Policlinico Universitario "A. Gemelli" IRCCS, 00168 Rome, Italy
14 Department of Biomedicine, Neuroscience and Advanced Diagnostics, Section of Radiology, University Hospital "Paolo Giaccone", 90127 Palermo, Italy; giuseppe.salvaggio@policlinico.pa.it
* Correspondence: viviana.benfante@arnascivico.it

Abstract: Background: Prostate cancer (PCa) is the second most common cancer in men, and radiotherapy (RT) is one of the main treatment options. Although effective, RT can cause toxic side effects. The accurate prediction of dosimetric parameters, enhanced by advanced technologies and AI-based predictive models, is crucial to optimize treatments and reduce toxicity risks. This study aims to explore current methodologies for predictive dosimetric parameters associated with RT toxicity in PCa patients, analyzing both traditional techniques and recent innovations. Methods: A systematic review was conducted using the PubMed, Scopus, and Medline databases to identify dosimetric predictive parameters for RT in prostate cancer. Studies published from 1987 to April 2024 were included, focusing on predictive models, dosimetric data, and AI techniques. Data extraction covered study details, methodology, predictive models, and results, with an emphasis on identifying trends and gaps in the research. Results: After removing duplicate manuscripts, 354 articles were identified from three databases, with 49 shortlisted for in-depth analysis. Of these, 27 met the inclusion criteria. Most studies utilized logistic regression models to analyze correlations between dosimetric parameters and toxicity, with the accuracy assessed by the area under the curve (AUC). The dosimetric parameter studies included Vdose, Dmax, and Dmean for the rectum, anal canal, bowel, and bladder. The evaluated toxicities were genitourinary, hematological, and gastrointestinal. Conclusions: Understanding dosimetric parameters, such as DVH, Dmax, and Dmean, is crucial for optimizing RT and predicting toxicity. Enhanced predictive accuracy improves treatment effectiveness and reduces side effects, ultimately improving patients' quality of life. Emerging artificial intelligence and machine learning technologies offer the potential to further refine RT in PCa by analyzing complex data, and enabling more personalized treatment approaches.

Citation: Piras, A.; Corso, R.; Benfante, V.; Ali, M.; Laudicella, R.; Alongi, P.; D'Aviero, A.; Cusumano, D.; Boldrini, L.; Salvaggio, G.; et al. Artificial Intelligence and Statistical Models for the Prediction of Radiotherapy Toxicity in Prostate Cancer: A Systematic Review. *Appl. Sci.* **2024**, *14*, 10947. https://doi.org/10.3390/app142310947

Academic Editors: Pedro Couto and Douglas O'Shaughnessy

Received: 16 October 2024
Revised: 18 November 2024
Accepted: 21 November 2024
Published: 25 November 2024

Keywords: artificial intelligence; deep learning; machine learning; predictive; radiotherapy; prostate cancer; toxicity; dosimetric

1. Introduction

Prostate cancer (PCa) [1–6] is the second most common cancer among men, with a significant impact on quality of life and mortality. Radiotherapy (RT) is one of the primary therapeutic options [7–12], offering significant benefits in local tumor control and survival [13–15]. Recent advances in medical imaging have significantly improved the accuracy and effectiveness of RT within the framework of precision medicine, making RT the most commonly used locoregional conventional cancer treatment [16–21].

Despite these advancements, toxicity-related side effects are a major concern for both patients and healthcare providers [22–27]. Dosimetric parameters play a pivotal role in predicting RT toxicity [28–34], as they determine the distribution of radiation dose within the target tissue and surrounding healthy tissue [35,36]. In order to maximize treatment efficacy while minimizing side effects, it is essential to accurately predict these parameters. A key component of recent RT progress has been the integration of advanced imaging techniques, optimization algorithms, and predictive models based on AI [37–42]. These innovations have transformed the field of biomedical analysis, enhancing segmentation [43–52], defining predictive models [53–64], and improving radiopharmaceutical distribution [65–70] and RT dosimetry [71–74]. These tools enable highly personalized treatment plans by adapting the dose distribution to the unique characteristics of each patient and their specific tumor [75–79].

However, the potential for toxicity ranging from acute to chronic effects remains a significant aspect of RT, often affecting patients' quality of life (QoL) [80–82]. Acute toxicity, occurring during or shortly after treatment, often involves urinary and gastrointestinal symptoms such as frequent urination, pain, and diarrhea, but these symptoms usually subside within weeks to months [80,83–86]. In contrast, late toxicity, which can develop months to years later, may cause more persistent problems, including urinary incontinence, chronic bladder irritation, bowel dysfunction, and erectile dysfunction [87–89].

The early identification and prediction of RT-inducted toxicity is therefore crucial to optimize treatment protocols and improve patients' QoL [90–94].

Smart healthcare, AI, and machine learning (ML) have transformed the medical field, particularly in cancer diagnosis and treatment. Historically, PCa management has progressed from basic screening methods in the early 20th century to advanced imaging and targeted treatments today. With the introduction of the prostate-specific antigen (PSA) test in the 1980s, early detection improved, although treatment options were still limited to surgery and traditional RT [95,96].

By the late 1990s, advances in RT allowed for more precise dose targeting, minimizing damage to surrounding tissue. The rise of AI and ML in the 2010s began a new era of predictive models, aiming to enhance patient outcomes by forecasting disease progression and personalizing treatment. Predictive RT, in particular, benefits from ML models trained on extensive datasets, enabling precise dose–volume histogram (DVH) predictions, toxicity outcomes, and personalized treatment adjustments [75].

In modern smart healthcare, wearable technology and AI-powered monitoring systems provide real-time patient feedback, making it possible to continuously refine treatments. As AI continues to develop, PCa care increasingly shifts toward precision medicine, leveraging complex algorithms to assess individual risk factors and optimize treatment plans, promising improved patient-specific outcomes in the near future. In recent years, research has focused on identifying predictors of RT toxicity, including clinical, dosimetric, and biological variables. The advent of advanced technologies, such as AI and ML, has further enhanced our ability to develop more accurate and reliable predictive models which can

help clinicians identify patients at high risk of side effects and modify treatment plans accordingly [62,75,76,97–101].

This review investigates methodologies for predicting dosimetric parameters in RT, particularly in PCa. It analyzes traditional techniques alongside recent innovations, including ML and AI, to assess the advantages, limitations, and clinical applications of these methods. The review also explores relationships between dosimetric parameters and clinical toxicity outcomes in organs at risk, such as the rectum, bladder, bowel, and bone marrow.

2. Materials and Methods

An extensive systematic literature review was conducted using the PubMed, Scopus, and Medline databases to define dosimetric predictive parameters for PCa-RT. Following the Preferred Reporting Items for Systematic Reviews and Meta-Analyses (PRISMA) recommendations [102], studies written in the English language and published between 1987 and April 2024 that addressed the prediction of dosimetric parameters of toxicity specifically in PCa RT were included in the analysis. The search strategy included the following specific keywords: "dosimetric", "predictive", "radiotherapy", "prostate cancer", "AI", "deep learning", and "machine learning".

2.1. Inclusion and Exclusion Criteria

The review included studies that addressed the following issues:

1. Predictive models for dosimetric parameters of toxicity in RT for PCa.
2. Clinical, dosimetric data, or AI techniques for prediction.
3. Conventional and moderate hypofractionated RT.

The following types of studies were excluded:

1. The ones that did not focus specifically on toxicity in RT for PCa.
2. The ones that did not focus on dosimetric data.
3. Those without experimental data, such as narrative reviews, letters to the editor, opinion articles, conference papers, or book chapters.
4. Those focused on Stereotactic Body Radiotherapy (SBRT) and brachytherapy (BT).

2.2. Data Extraction

For each included study, the following data were extracted:

1. General Information: first author, year of publication, DOI (Digital Object Identifier).
2. Methodology: number of patients, anatomical district, imaging techniques used, dosimetric parameters analyzed.
3. Predictive Models: Type of used model, software, predictive parameters, presence or absence of a public dataset, type of images used.
4. Results: performance evaluation indexes, predictive dosimetric parameters with possible clinical applications.

2.3. Data Analysis

Analyses of the extracted data, shown in Table 1, were conducted both qualitatively and quantitatively. A summary of the characteristics of the included studies and their key findings was provided. In addition, emerging trends and gaps in the existing literature were identified. The data reported in the table include the title of the paper, the name of the first author, the year of publication, the DOI, the anatomical site, the number of patients included in the study, the method employed for statistical analysis, the formula used, the software used, the indices for evaluating the performance of the method, the presence of a public dataset, which type of images were used, the dosimetric parameters analyzed, and the main findings of the study.

Table 1. Characteristics of studies in growing order of date.

Study	N of Patients	Method	Software	Valuation Index	Analyzed Parameters	Findings
Fiorino C. et al. 2002 [103]	402	Cox regression model	Statistica (StatSoft Inc., Tulsa, OK, USA)	*p*-values were used to evaluate correlations	Rectum Dmax, Dmean, V50–75 Gy	V50 < 60–65%, and V60 < 50–55% seem to be the robust cut-off values to keep the risk of developing late rectal bleeding reasonably low
Cozzarini C. et al. 2003 [104]	154	Cox regression model	Statistica (StatSoft Inc.)	*p*-values were used to evaluate correlations	Rectum Dmean, V50–65	V50 > 63% for bleeding
Fiorino C. et al. 2003 [105]	245	Cox regression model	Statistica (StatSoft Inc.)	Hazard Ratios (HR) with ROC curves	Rectum V50–70	To keep the rate of moderate/severe rectal bleeding < 5–10%, it seems advisable to limit V50 to 60–65%, V60 to 45–50%, and V70 to 25–30%
Zapatero A. et al. 2004 [106]	107	Univariate logistic regression	Statistical Package for Social Sciences, version 10.0	AUC = 0.89	Rectum Dmax, Dmean, V30–V72	G2 rectal bleeding Dmean < 50.0 Gy and V60 < 42%
Fiorino C. et al. 2008 [107]	1132	Logistic regression analysis	FORTRAN (IBM, Armonk, NY, USA)	HR and *p*-values were used to evaluate correlations	Rectal V20–V75 Gy	Fecal incontinece V40 < 75%; V70 for bleeding G2; V75 for bleeding G3
Arcangeli S. et al. 2009 [108]	102	Logistic regression analysis	n.a.	Odds Ratios (ORs) were used to evaluate correlations	Rectal V50, V53	Rectal G2 toxicity for V53 > 8%
Faria S. et al. 2010 [109]	71	Multivariable logistic model	n.a.	*p*-values were used to evaluate correlations	Rectum and the rectal wall: Dmax, Dmean, D50%, D25%	No relationship between these constraints and late rectal toxicity
Perna L. et al. 2010 [110]	96	Multivariable logistic regression	MedCalc (Ostend, Belgium)	AUC = 0.64	DVH of Intestinal Cavity and of the loops	V45 TL > 50 cc, V50 TL > 13 cc, V55 TL > 3 cc
Tomita N. et al. 2013 [111]	241	Multivariable logistic regression	n.a.	*p*-values were used to evaluate correlations	Rectum covered by 70 Gy (V70), 60 Gy (V60), 40 Gy (V40), and 20 Gy (V20)	Rectum Dmax, V70 and V60 of the ≥ GI Grade 2
Norkus D. et al. 2013 [112]	124	Logistic regression analysis	StatView (SAS Institute Inc., Cary, NC, USA)	*p*-values were used to evaluate correlations	Rectal volume, bladder volume, rectal and bladder dose/volume cut-points (V40 Gy/V33 Gy, V50 Gy/V42 Gy, V60 Gy/V50 Gy, V70 Gy/V58 Gy, and V76 Gy/V63 Gy	No parameters were significant
Viani G.A. et al. 2013 [113]	217	Logistic regression analysis	SPSS version 19	ORs were used to evaluate correlations	Rectum, bladder Vdose, femur Dmax	No significant dosimetric predictors
Ippolito E. et al. 2013 [114]	101	Logistic regression	SPSS (v.16, Chicago, IL, USA)	AUC > 0.6	Rectum Dmax, Dmean, V50–70 Gy	V60 Gy < 34.4%, rV70 Gy < 16.7%, rDmean < 57.5 Gy
Kong M. et al. 2014 [115]	70	ROC curves analysis	SPSS version 18.0 (IBM Corporation, Armonk, NY, USA)	AUC	Rectum and bladder Dmax, V5–75	Rectum: max dose 76.5 Gy Bladder: V40 to 17.3% and V50 to 10.2%
Jin-Hong Park et al. 2014 [116]	92	Univariate logistic regression	SPSS version 20.0	AUC > 0.65	Trigone, bladder, wall bladder V15-V50	G2 GU toxicity for bladder V20

Table 1. *Cont.*

Study	N of Patients	Method	Software	Valuation Index	Analyzed Parameters	Findings
Sini C. et al. 2015 [117]	121	Logistic regression analysis	R (R Core Team Vienna, Austria)	AUC = 0.904	Bone marrow V3–50 Gy	WP-V40 > 599 cc for G3 acute lymphopenia; IL-V40 > 95 cc for G2 late lymphopenia
Cozzarini C. et al. 2015 [118]	262	Logistic regression	KNIME (KNIME GmbH, Konstanz, Germany), R 2.15.2	AUC > 0.6	Absolute weekly bladder dose–surface histograms	Frequency, intermittency, urgency, and nocturia absolute weekly bladder DSH > 5 Gy/11.5 Gy/ 12.5 Gy week
Stankovic V. et al. 2016 [119]	94	Logistic regression analysis	n.a.	OR and *p*-values were used to evaluate correlations	Rectum Dmax, Dmean, V50–72 Gy	GI acute grade ≥1 for V50–72
Bagalà P. et al. 2016 [120]	86	Cut-off volume model of NTCP to fit bladder late toxicity data	R version 2.15.1, MATLAB 2008b version 7.7 (MathWorks, Natick, MA, USA).	*p*-values were used to evaluate correlations	Bladder and bladder inferior V65 < 50%, V70 < 35%, V75 < 15%, and V80 < 15%	Strong association between high doses (>77 Gy) and late GU toxicity
Son C.H. et al. 2016 [121]	87	Generalized estimation equations (GEEs)	n.a.	OR = 0.82	Bladder V70 Gy and penile bulb V70 Gy	Bladder V70 Gy was independently associated with a decrease in urinary continence scores
Arunsingh M. et al. 2017 [122]	101	Logistic regression	n.a.	AUC = 0.70	Rectal V50–70; Bladder V65–70	Rectal G2 toxicity: VEQD2–60 Gy > 9.7 cc; VEQD2–50 Gy > 15.9 cc
Katahira-Suzuki R. et al. 2017 [123]	82	ROC curves and Youden Index	SPSS version 22, (IBM, Chicago, IL, USA)	OR and *p*-values were used to evaluate correlations	Rectum Dmax, Dmean, V30–76 Gy	V30, V40, V50, and V60 were significant predictors for G ≥ 1 late rectal bleeding; rectal V30 and V40 were predictive factors for G2
Mostafaei S. et al. 2019 [124]	64	Stacking algorithm and elastic net penalized logistic regression	itk-SNAP, Python	Hosmer–Lemeshow test, AUC = 0.77	Rectum, bladder, rectal and bladder walls D5–D95 and V5–V75 Gy	CT imaging features could predict radiation toxicities and combination of imaging and clinical/dosimetric features may enhance the predictive performance of radiotoxicity modeling
Peng X. et al. 2019 [125]	248	Logistic regression models	n.a.	AUC = 0.653	Anal canal Dmax, Dmean, V10–70 Gy	Anal canal V20 > 74.93%
Catucci F. et al. 2021 [126]	175	Univariate logistic regression analysis	R (R statistical software version 3.3.1, R Core Team Vienna, Austria)	AUC = 0.626	Vdose	GU toxicity ≥ G2 related to V51 (%)
Bresolin A. et al. 2021 [127]	415	Multivariate logistic regression	R version 3.2.4	Hosmer–Lemeshow test and AUC (0.63–0.67)	DVHs of bowel loops	Bowel loops (V46 < 80 cc) may reduce the risk of G2-G3 intestinal symptoms
Ong L.K.A. et al. 2022 [128]	150	Univariate logistic analysis	SPSS v27.0. and R version 4.0	AUC ≥ 0.6	Rectum Dmean, D0.003 cc, V30–75 Gy	Rectal G2 toxicity for D0.03 cc ≥ 78.2 Gy
Fenlon J. B. et al. 2024 [129]	203	Nonparametric kernel regressions	STATA version 16	n.a.	Bone marrow 500, 1000, 1500, 2000, and 2500 cc	>1000 cc of bone marrow receiving ≥15 Gy had significantly lower predicted Hb

3. Results

After removing duplicate manuscripts, a total of 354 manuscripts were identified from the 3 databases. After the first screening, 305 papers were excluded, as the title and abstract were considered not relevant to the topic. Forty-nine papers were shortlisted for extensive analysis. Sixteen of these were excluded from the search, as they did not focus on dosimetric data for RT toxicity prediction in PCa, and a further 6 because they were articles on SBRT and BT. The remaining 27 articles were reviewed, as they fulfilled the inclusion criteria [103–129]. Figure 1 describes the PRISMA workflow.

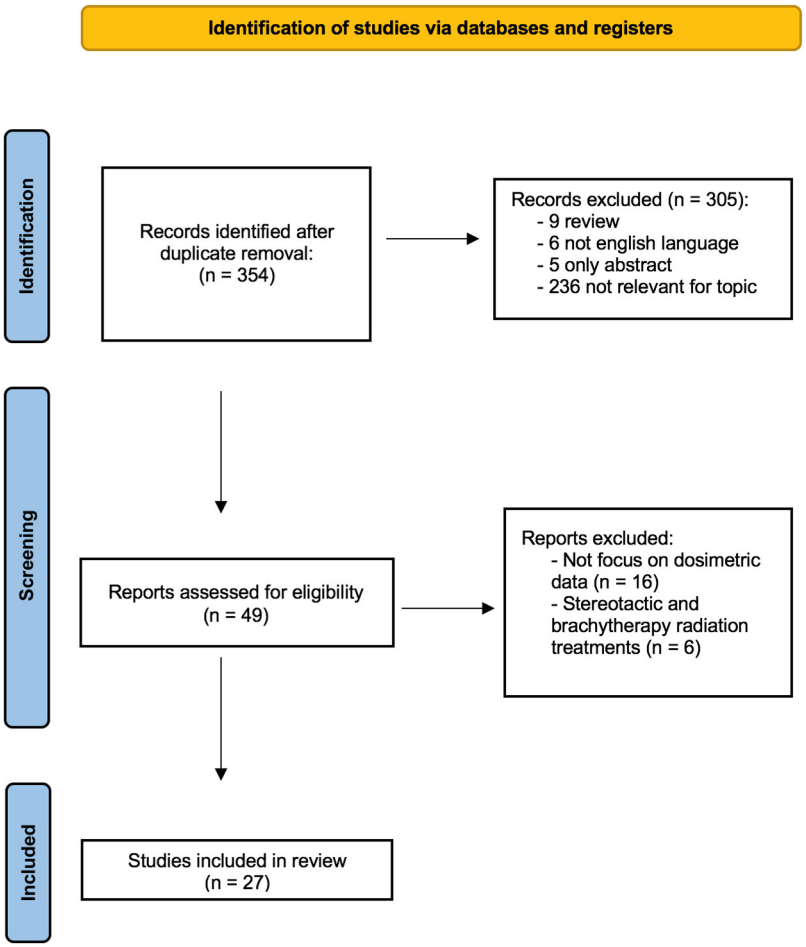

Figure 1. PRISMA flow diagram.

In the majority of the reviewed studies, a logistic regression model was used to determine correlations between dosimetric parameters and side effects.

Commonly used software for statistical analysis includes R and FORTRAN. The accuracy of predictive models was determined by performance indices with area under the ROC curve (AUC) [130] values ranging from 0.626 to 0.904.

Only one study implemented ML techniques to enhance predictive accuracy [124].

Several dosimetric parameters were analyzed, such as the volume receiving a certain dose (Vdose), maximum dose (Dmax), and mean dose (Dmean), primarily focusing on the rectum and bladder.

The studies reported dosimetric parameters that were predictive of genitourinary (GU), haematological, and gastrointestinal (GI) toxicity.

3.1. Genitourinary Toxicity

The occurrence of GU toxicities during RT for pelvic region cancers has an impact on both patient tolerance to treatment and accuracy of dose delivery. On the one hand, urinary symptoms impact patients' QoL, restricting their ability to perform daily activities [89]. On the other hand, RT-induced incontinence complicates the maintenance of adequate bladder filling during treatment, resulting in the need for re-optimization for adequate target coverage [131].

In response to these challenges, multiple studies have focused on establishing validated dosimetric constraints to predict the onset of GU toxicity in PCa RT.

A retrospective study from the University Medical center of Seoul in 2014 analyzed acute and late toxicities in 70 patients with localized PCa treated with hypofractionated helical tomotherapy [115]. RT protocol included doses of 75 Gray (Gy) in 2.5 Gy per fraction to the prostate gland, 63 Gy in 2.1 Gy per fraction to the seminal vesicles, and 54 Gy in 1.8 Gy per fraction to the pelvic lymph nodes. The findings revealed that acute gastrointestinal (GI) toxicity occurred in 51.4% of patients at grade 0, 42.9% at grade 1, and 5.7% at grade 2, while acute genitourinary (GU) toxicity was noted in 7.1% at grade 0, 64.3% at grade 1, and 28.6% at grade 2. Significant predictive factors for severe toxicities included maximum rectal dose and bladder V40 and V50. The analysis showed a significant correlation between bladder toxicity onset and values of bladder V40 > 17.3% and V50 > 10.2%, where Vx is the volume of tissue receiving at least x Gy. The results from Kong et al. [115] were similar to the outcomes reported in the study by Catucci et al. (2021) [126]. The authors analyzed a cohort of 175 patients and found a significant correlation between bladder G $\geq$ 2 late toxicity and a bladder Vdose of 51 Gy.

Jin-Hong-Park et al. (2014) conducted a prospective study to investigate the occurrence of acute bladder toxicity following pelvic RT and identified potential dosimetric predictors [116]. Acute bladder toxicity was assessed weekly using the Common Terminology Criteria for Adverse Events (CTCAE version 4.0). The reported symptoms were also rated according to the International Prostate Symptom Score (IPSS) and the Overactive Bladder Symptom Score (OABSS) to provide a comparative analysis of different toxicity metrics. The study involved the delineation of the bladder wall, solid bladder, and trigone on CT scan planes, followed by analysis of dose–volume histograms to identify the most reliable predictors. A total of 92 patients were included in the analysis, and 27 patients (29%) showed CTCAE G2 acute bladder toxicity, with nocturia as the most prevalent symptom. V20 for both the bladder wall and the whole bladder had a higher predictive value for bladder toxicity. The IPSS was found to be more aligned with CTCAE than OABSS for toxicity reporting [116].

A prospective trial conducted by Cozzarini C. et al. (2015) developed an alternative predictive tool for bladder toxicity [118]. The bladder dose–surface histograms (DSHw) were weekly reported as dosimetric descriptors in 262 PCa patients treated with RT (120 conventional fractionation, 142 hypofractionation). The authors found that GU toxicity in terms of increased risk of frequency, intermittency, urgency, and nocturia was significantly associated with DSHw values. DSH is an RT evaluation tool that quantifies the distribution of radiation dose across the surface of the bladder. Unlike traditional dose–volume histograms (DVH), which assess the dose delivered to the entire volume of an organ, the DSH specifically focuses on the dose distribution along the organ's surface.

Bagalà P. et al. (2016) retrospectively analyzed the relationship between GU toxicity and clinical dosimetric parameters in 86 PCa patients treated with conformal RT [120]. They found a strong association between high doses (>77 Gy) in the bladder and late GU toxicity. Similar results were reported in a study by Son C.H. et al. (2016) with urinary continence scores correlated with bladder V70 Gy [121].

3.2. Haematological Toxicity

Bone marrow irradiation in pelvic RT has been already addressed as a relevant factor promoting haematological toxicity in different subsites [132,133]. Indeed, dose optimization

should also be considered in PCa RT [117]. Sini et al. (2015) conducted a study to identify clinical and dosimetric predictors of acute and late hematologic toxicity (HT) in chemo-naïve patients undergoing whole-pelvis radiotherapy (WPRT) for PCa. By Analyzing data from 121 patients treated with various RT techniques (static-field IMRT, VMAT/Rapidarc, and tomotherapy), the researchers delineated pelvic bone marrow (BM) into specific regions and calculated their dose–volume histograms (DVHs). Significant differences in BM DVH were found among the treatment techniques, with tomotherapy associated with larger volumes receiving lower doses and smaller volumes receiving higher doses. Lower baseline absolute counts of white blood cells, neutrophils, and lymphocytes were identified as strong predictors of acute and late HT. It was found that higher BM volumes receiving 40 Gy (V40) were associated with increased risks of acute Grade 3 and late Grade 2 lymphopenia. The study developed two predictive models, which incorporated baseline absolute lymphocyte counts and specific BM dose constraints, showing promising areas under the curve (AUC) for predicting lymphopenia. These findings suggest that targeted dose constraints to pelvic BM can help mitigate hematologic toxicity, thereby potentially improving patient outcomes.

Also, Fenlon J. B. et al. (2024) performed a prospective data collection of PCa patients undergoing RT [129]. The results showed that a bone marrow volume > 1000 cc receiving $\geq$ 15 Gy correlates with significantly lower predicted hemoglobin levels. Plan optimization considering the further mentioned value did not affect target coverage in the selected series.

3.3. Gastrointestinal (GI) Toxicity

The onset of GI toxicity is a main concern in PCa RT due to the anatomical proximity of the prostate to the rectum and other parts of the gastrointestinal tract. GI toxicity includes a range of symptoms, including diarrhea, tenesmus, rectal pain, rectal bleeding, and, in some cases, proctitis. The possibility of identifying predictive parameters for different GI subsites and symptoms has been investigated [134].

The necessity to limit radiation exposure to the bowel to prevent intestinal side effects has been well established. In this regard, this review highlights two significant studies that suggest specific dose limits to mitigate radiation-induced bowel toxicity. The first study, conducted by Perna L. et al. in 2010, involved a retrospective analysis of 96 patients who underwent whole pelvis irradiation after prostatectomy. The findings revealed a correlation between acute bowel toxicity and certain dose–volume thresholds, specifically for V45 total loops (TL) > 50 cc, V50 TL > 13 cc, and V55 TL > 3 cc [110].

Similarly, a more recent study by Bresolin A. et al. in 2021 analyzed data from 415 patients enrolled in a multi-institutional prospective trial. This study suggested that keeping bowel loops at V46 below 80 cc could potentially reduce the risk of developing G2 to 3 intestinal symptoms [127].

Considering rectal toxicity, different experiences searched for dosimetric parameters. In a prospective trial, Arcangeli et al. (2009) evaluated clinical and dosimetric predictors of acute toxicity after hypofractionated RT in 102 patients affected by PCa [108]. The results of this study showed a correlation between G2 rectal toxicity at rectum V53 > 8%.

Ippolito E. et al. (2013) performed a prospective analysis on patients treated for exclusive and adjuvant RT with a 1-year colonoscopy to identify rectal telangiectasia [114]. The authors correlated the onset of rectal telangiectasia (showed at endoscopic examination) with rectal V60 Gy < 34.4%, rectal V70 Gy < 16.7%, and rectal Dmean < 57.5 Gy.

3.4. Rectal Bleeding

Fiorino et al. conducted three studies, and the author investigated predictors of late rectal toxicity in PCa patients treated with three-dimensional conformal RT (3D-CRT). In the first study, dose–volume histogram (DVH) data from 245 patients showed substantial correlations between rectal bleeding and dose thresholds (V50-V70), recommending constraints at V50 $\leq$ 60–65%, V60 $\leq$ 45–50%, and V70 $\leq$ 25–30% to decrease bleeding risk. The second study, focusing on post-radical prostatectomy patients, identified significant DVH thresholds for late hematuria and rectum hemorrhage, specifically bladder V50 Gy

≤ 43%, bladder V40 Gy ≤ 50%, rectum V60 Gy ≤ 13%, and rectum V50 Gy ≤ 33%. In the third study, which included 506 patients with a 24-month follow-up, multivariate analysis confirmed dose–volume constraints as predictors of rectal toxicity, with V70 being highly predictive of bleeding (recommended V70 < 25%), and previous abdominal/pelvic surgery strongly correlating with stool frequency, pain, incontinence, and bleeding. For patients with surgery history, a more stringent V70 threshold (<15%) was advised. Together, these studies highlight specific dose constraints and patient history factors critical for managing late rectal toxicity in PCa RT [103,105,107].

Further experiences also confirmed the reported dose limits for rectal toxicity, which are summarized in Table 1 [104,106,111,115,119,122,123,128].

3.5. Anal Toxicity

Peng X. et al. (2019) conducted a study to evaluate the clinical and dosimetric factors predictive of acute anal toxicity (AAT) following RT in PCa patients, both with and without hemorrhoids [125]. They analyzed data from 347 PCa patients treated with pelvic RT at a single institution, comprising 248 cases treated from July 2013 to November 2017 as the training cohort and 99 cases treated in 2018 as the validation cohort. The prescribed dose was determined using the anal canal dose–volume histogram. Univariate and multivariate analyses were conducted to evaluate AAT risk based on clinical and dosimetric factors. The results indicated that 39.5% (98/248) of patients in the training cohort and 31.3% (31/99) of patients in the validation cohort developed AAT. The incidence of AAT was significantly higher in patients with hemorrhoids than in those without hemorrhoids in both cohorts. Hemorrhoids and volume receiving more than 20 Gy (V20) were identified as independent factors for predicting AAT in the training cohort, with similar results observed in the validation cohort. The combination of hemorrhoids and a high anal canal V20 (>74.93% as determined by ROC curves) demonstrated the highest specificity and positive predictive values for predicting AAT in both cohorts. The study concluded that AAT is common in PCa patients with hemorrhoids during and after pelvic RT. Hemorrhoids and anal canal V20 are independent predictors of AAT, and these factors should be carefully considered during treatment planning to minimize AAT incidence. The authors also found that acute toxicity in the anal canal is correlated with anal canal V20 > 74.93%, and suggested to keep the rate of moderate/severe rectal bleeding below 5–10%; it seems advisable to limit V50 to 60–65%, V60 to 45–50%, and V70 to 25–30%.

The studies by Farìa [109], Norkus [112], and Viani [113] did not demonstrate statistically significant correlations between dosimetric parameters and side effects.

All included studies did not contain public datasets.

4. Discussion

An accurate understanding of dosimetric parameters and their correlation with toxicity is crucial for optimizing RT plans. Improving toxicity prediction can lead to more effective treatment tailoring, minimizing adverse effects and improving patients' QoL.

Furthermore, the identification of key dosimetric parameters can guide future research and development of advanced RT techniques [135].

We are aware of the main dosimetric parameters, such as the DVH, Dmax and Dmean, conformity, and Gamma Index [136,137].

The DVH is a fundamental tool that shows the relationship between the received dose and the volume of irradiated tissue. Two of the main parameters extracted from the DVH are Vx and Dx (dose received in x% of tissue volume). The Dmean and Dmax are used to assess the radiation load on tissue [138]. Figure 2 illustrates a DVH sample in an RT of PCa to highlight the relationship between dosimetric parameters like the Dmean, Dmax, and Vdose with toxicity outcomes.

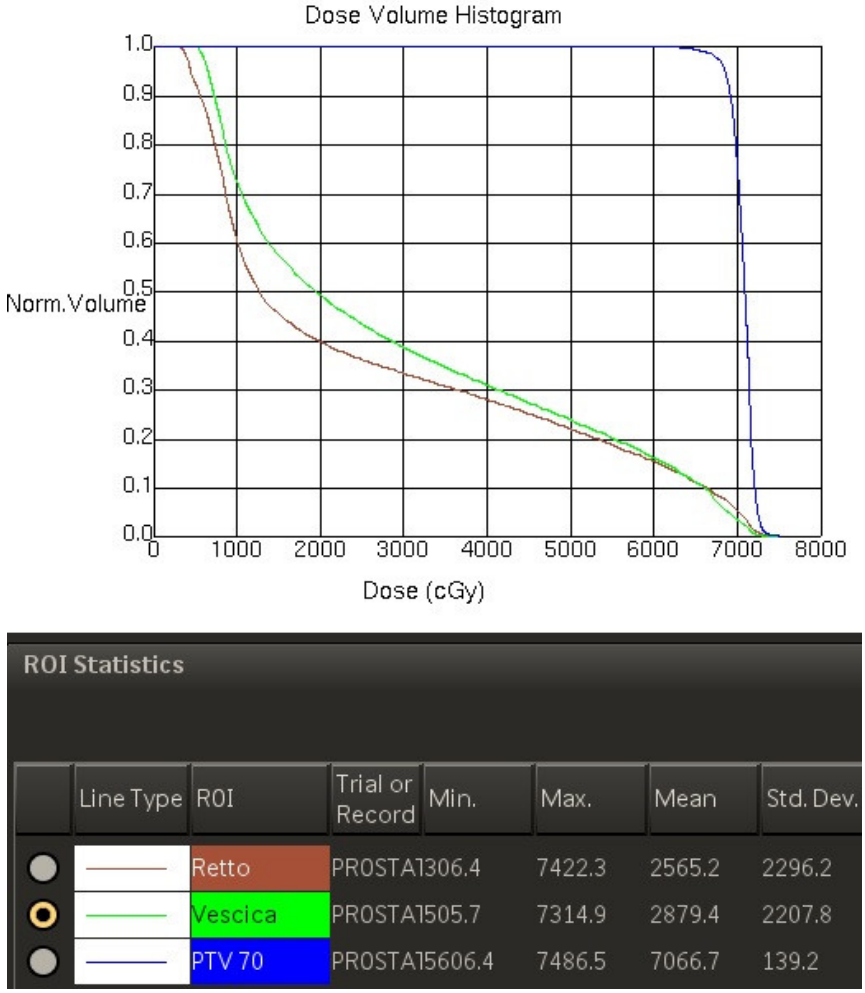

Figure 2. RT of PCa using a DVH sample.

- Dmean: A higher Dmean in organs at risk may correlate with increased toxicity; thus, it is crucial to minimize this value.
- Dmax: Identifying the Dmax helps in understanding potential hotspots that could lead to adverse effects.
- Vdose: Higher Vdose values (e.g., V50 > 50% of the rectum receiving more than 50 Gy) often correlate with increased risk of toxicity.

Haemorrhagic cystitis can occur as a result of high doses given to the bladder in the context of the prostate. In contrast, a high maximum dose to the rectum may increase proctitis risk [136].

The conformity index (CI) measures how well the irradiated dose matches the tumour target shape while minimizing exposure to surrounding healthy tissue. A high CI indicates effective compliance, reducing the risk of damage to non-target tissues [139].

The Gamma Index is used to assess the quality of the treatment plan by comparing the planned dose with the delivered dose. Significant discrepancies may indicate an increased risk of toxicity, as tissue may receive unplanned doses [140].

This review provides a comprehensive overview of the dosimetric parameters used to predict toxicity in PCa RT, highlighting key correlations and the most effective methodologies.

Almost all studies included in this review use logistic regression analysis as a well-established method, which helps determine the probability of toxicity events. Logistic regression models are particularly effective for straightforward yes-or-no outcomes, making them ideal for assessing whether specific thresholds of radiation exposure (e.g., rectum V50 or bladder V70) increase the odds of developing a certain grade of toxicity. For instance,

the study by Arunsingh et al. (2017) showed that increased rectal volume exposed to 60 Gy was a strong predictor of Grade 2 acute toxicity [122]. Meanwhile, Sini et al. (2016) demonstrated that bone marrow exposure levels could accurately predict hematologic toxicity with high AUC values, reinforcing the model's accuracy [117]. In cases where the timing of toxicity onset is important, such as when assessing the risk of late GU toxicity over several months or years, studies used the Cox proportional hazard model. This approach allowed researchers to analyze not just the likelihood of toxicity but also when it was likely to develop after treatment. For example, Kong et al. (2014) used Cox regression to explore bladder and rectal dose levels in hypofractionated treatments, finding that certain dose–volume constraints could help reduce the risk of delayed toxicity [115]. Similarly, Fiorino et al. (2008) employed Cox regression to investigate rectal dose thresholds, confirming that limiting rectum V70 to lower levels could mitigate the long-term risk of severe rectal bleeding [107].

Another statistical tool applied in these studies is the Generalized Estimating Equation (GEE), which is particularly helpful for tracking repeated measures over time, such as patient-reported outcomes (PROs) on urinary or bowel function. The longitudinal perspective of GEEs allows for insights into how symptoms might change after treatment, providing a dynamic view of toxicity progression. For example, Son et al. (2016) used GEEs to analyze how continence scores evolved over time, showing that higher bladder V70 volumes significantly correlated with deteriorating urinary function [121].

Only one study went beyond traditional statistical methods, applying ML techniques for enhanced predictive accuracy. Techniques like stacking ensembles, which integrate multiple models such as support vector machines and random forests, allow for a more complex analysis of toxicity risk by incorporating a broader array of clinical, dosimetric, and even radiomic data. Mostafaei et al. (2019), indeed, applied a stacking ensemble to predict urinary toxicity with high precision, underscoring the potential of ML to refine toxicity prediction in cases where conventional models may fall short [124].

The process began with three different ML algorithms, or "base models", with each analyzing radiomic data derived from pre-treatment CT scans. A random forest model was used to capture complex, non-linear patterns, taking advantage of its ability to manage intricate datasets and detect subtle variations in tissue characteristics. Alongside it, a support vector machine (SVM) contributed its strength to handling high-dimensional data—a necessary skill given the detailed, feature-rich radiomic inputs. Lastly, a neural network was included to detect finer, subtle patterns within the tissue structure, which was especially useful for understanding the small-scale changes caused by radiation.

After each base model analyzed the data and made its own predictions, a final layer, known as the meta-learner, brought these insights together. The researchers chose elastic net penalized logistic regression for this role, as it is particularly effective at selecting the most relevant features and balancing them for optimal performance. This choice allowed the meta-learner to focus on the most meaningful radiomic, clinical, and dosimetric features, filtering out any less important details to avoid overfitting and improve the model's generalizability. To ensure the model's reliability, the team implemented cross-validation, dividing the data into multiple parts to test and refine the model across different data splits. This method strengthened the model's consistency, ensuring it would perform reliably even when applied to new patients.

The results were encouraging: by combining the radiomic, clinical, and dosimetric data, the stacking model reached an impressive accuracy level, with an AUC of 0.77 for urinary toxicity prediction. This performance was notably higher than models using only clinical or dosimetric information, underscoring the additional predictive power that radiomic features bring. The study concluded that integrating machine learning into toxicity prediction models offers a significant step toward personalized RT, allowing clinicians to identify patients at higher risk of treatment side effects and potentially adjust treatment plans accordingly.

In essence, Mostafaei et al.'s study highlights how a sophisticated machine learning approach can offer deeper insights into patient-specific responses to RT, paving the way for more individualized, safe, and effective cancer treatments.

To assess the reliability of these models, various performance metrics were employed, each with its own strengths and limitations. One of the most commonly used metrics is the AUC from ROC analysis, which measures a model's ability to distinguish between patients who will and will not experience toxicity. An AUC close to 1 signals a high level of accuracy in the model's predictions. This metric was used extensively across studies to confirm DHV threshold predictive power; for instance, Zapatero et al. (2004) achieved AUC values as high as 0.89 when predicting rectal bleeding, suggesting that specific dose constraints could reliably prevent such toxicity [106].

While the AUC focuses on the model's discriminative power, Odds Ratios (ORs) derived from logistic regression provide an interpretable measure of the increased risk associated with specific DVH values. For instance, Cozzarini et al. (2002) reported that a rectal V50 above 63% increased the odds of late rectal bleeding significantly, making this threshold a practical guide for clinicians. ORs have the advantage of directly quantifying risk in an easily understandable format, allowing dose adjustments in clinical settings [104].

Calibration plots and the Hosmer–Lemeshow test offer a way to ensure that a model's probability predictions align with actual outcomes. Calibration plots visually compare predicted probabilities with observed results, while the Hosmer–Lemeshow test statistically confirms this fit. Studies like Catucci et al. (2021) found calibration plots useful in validating their bladder toxicity predictions, helping fine-tune the model to match real-world occurrences [126]. Bresolin et al. (2021) also leveraged calibration plots to confirm that their bowel toxicity predictions aligned well with observed data, thus validating the chosen DVH constraints [127].

In some cases, studies employed bootstrap validation to enhance model stability confidence. By repeatedly sampling from the dataset, bootstrap validation tests the model's robustness and reduces the risk of overfitting, which is especially valuable in studies with smaller patient cohorts. For instance, Catucci et al. (2021) used bootstrapping to confirm the stability of their bladder toxicity model, ensuring that the AUC and other metrics remained consistent across samples [126].

Traditional models (Logistic Regression, Cox, GEE) offer interpretable predictions using established statistical methods, excelling with binary outcomes or time-to-event data but often faltering with complex, non-linear relationships. ML models, in contrast, handle high-dimensional, non-linear data and offer greater predictive power, but require complex data processing and stringent validation to avoid overfitting. Validation metrics like AUC, ORs, calibration plots, and bootstrap methods assess model accuracy and reliability. Overall, while traditional models are valued for interpretability, ML techniques are advancing predictive accuracy and supporting personalized approaches in RT.

Studies using AI will certainly be published within the next few years in order to predict dosimetric parameters. Indeed, AI and ML are emerging powerful tools for predicting toxicity. Such models are able to analyze large amounts of dosimetric, clinical, and multiomics data to identify complex patterns that predict toxicity [141–143].

Some approaches include regression models, used to identify linear relationships between dosimetric parameters and toxicity outcomes; artificial neural networks, used to analyze non-linear and complex data, improving predictivity over traditional models; and random forests and Gradient Boosting, i.e., Ensemble Learning Techniques that combine multiple predictive models to improve prediction accuracy [144,145].

In our research, we found several studies reporting the use of AI tools for the prediction of toxicity in RT treatment in patients with PCa, but they were not included as they did not provide specific predictive dosimetric parameters.

For example, Isaksson et al. [75] investigated toxicity outcomes in PCa RT, focusing on erectile dysfunction (ED), GI, rectal, and GU toxicities. Various ML models were employed,

including SVMs, artificial neural networks (ANNs), and random forests (RFs), to predict these effects using datasets ranging from 79 to 754 patients.

Some studies also explored genetic and radiomic markers. For instance, Lee et al. [146] used gene ontology to link neurogenesis and ion transport to urinary functions, while Abdollahi et al. [147] examined MRI radiomic features to predict toxicity. ANN and logistic regression models were common approaches, as seen in Carrara et al. and Moulton et al. [148,149], who found spatial dose distribution to be crucial for reducing GI toxicity. Other advanced methods included independent component analysis (ICA), as in Fargeas et al. [150], and tensor decomposition by CP-DMA.

Incorporating clinical, dosimetric, and radiomic data often enhanced predictive accuracy. Abdollahi et al. [151], for instance, combined MRI features to improve early rectal toxicity predictions.

Yahya et al. [62] explored a variety of statistical learning strategies to predict urinary symptoms following RT in PCa, each with unique strengths for handling complex datasets. Logistic regression, a widely used approach to binary outcomes, was refined through backward stepwise feature elimination based on Akaike Information Criterion (AIC) values to ensure only the most relevant predictors remained. Elastic-net, a method combining lasso and ridge regression, was particularly useful for managing datasets with correlated features, as it both selects important variables and balances their influence. Random forest, an ensemble technique, creates a robust prediction model by merging results from multiple decision trees, thereby reducing overfitting and enhancing accuracy. Neural networks, composed of interconnected input, hidden, and output layers, were optimized to identify nonlinear relationships and model complex patterns within the data. SVMs, with their ability to identify an optimal boundary between two classes, utilized a radial basis function kernel to handle nonlinearity effectively. Finally, MARS (Multivariate Adaptive Regression Splines) generated segmented, localized models that adapted to the data's unique structure, simplifying the overall model while retaining accuracy through a pruning process that minimizes irrelevant features. Each of these strategies was fine-tuned using cross-validation to improve prediction robustness and relevance.

An example of a recent paper that uses AI for this purpose is the study by Xiaoying Pan et al. [152] in 2020. They utilized ensemble ML to interrogate the entire DVH to evaluate the relationships between dose–volume parameters and patient-reported health-related QoL changes. They applied ensemble learning methods, which combine multiple weak models, to improve prediction accuracy and robustness. They tested two main types: random forest, which builds multiple decision trees on random subsets, and boosting, which incrementally corrects errors. For boosting, we used Gradient Boosting Decision Trees (GBDT) and Adaptive Boosting, with GBDT building each tree to minimize prior errors.

The ROC curve is widely recognized as a reliable tool for assessing binary classifiers' performance. However, caution is needed when applying it to imbalanced datasets. Alternatives like concentrated ROC (CROC), Cost Curves (CCs), and Precision–Recall plots (PRCs) have been proposed, although they are less common. Many studies still rely on ROC for performance evaluation, even with imbalanced data. Saito et al. [153] propose that PRC plots, unlike ROC, visually highlight classifier sensitivity to imbalance and offer a straightforward, accurate interpretation of practical performance. Their findings strongly suggest that PRC plots are the most informative tool for visual performance analysis.

The integration of advanced technologies, such as image-guided radiotherapy (IGRT) and intensity-modulated radiotherapy (IMRT), together with an in-depth understanding of dosimetric parameters, represents the future path to safer and more personalized RT treatment of PCa [79,154].

Although public datasets are missing and there is a lack of method details in some studies that hamper the replicability and independent verification of results, the use of advanced software and robust statistical models, such as logistic regression analysis, contributes to the validity of results [62].

The topic of this review focused on RT with conventional fractionation, while many screened and rejected studies were aimed at ultra-fractionation and brachytherapy treatments, so it would be useful to perform reviews with these two topics to possibly find innovative applications of AI in finding predictive dosimetric parameters in such increasingly popular care.

Applications of AI in the prediction of toxicity and outcomes of RT treatments represent a rapidly evolving area of medicine [155–158].

RT practitioners may hesitate to adopt AI models that operate as "black boxes", as this lack of transparency can undermine trust in AI-driven decisions. To build radiation oncologists' trust, it is essential to promote transparency by explaining how AI models work, using feature importance and visualization tools. Additionally, clarifying that AI is a supportive tool, with final decisions always resting with the physician, reinforces their role in patient care. Allowing oncologists to adjust potential AI errors not only enhances patient safety but also contributes to refining the AI model itself, improving its accuracy over time. Sharing case studies that showcase AI's positive impact and involving radiation oncologists in the development process further fosters understanding, while providing targeted training empowers practitioners to confidently integrate AI into their workflows [159,160].

Future trends in advanced medical technology focus on large language models (LLMs) and digital twins, which hold transformative potential for healthcare. LLMs can enhance diagnostics, treatment personalization, and patient education, while digital twins—virtual models of patients—could enable real-time monitoring, predictive analyses, and tailored interventions, pushing precision medicine forward [161–163].

In the future, these applications could have a significant impact in several ways. AI has the capability to analyze large amounts of clinical data and medical images to identify patterns and predict how patients will respond to specific treatments. This analysis could enable physicians to tailor plans to each patient's individual characteristics, thereby improving treatment effectiveness and reducing toxicity. AI can help optimize RT doses, balancing treatment efficacy with toxicity risk. This can lead to better tumor control and reduced side effects [164,165].

AI systems can be employed to monitor patients in real-time during RT delivery, facilitating the detection of changes in treatment response and allowing timely adjustments to the treatment plan [79].

In RT prediction, balancing model complexity and real-time performance is essential. While complex models like deep neural networks offer higher accuracy, they demand more computational resources and longer processing times, which can delay clinical decisions. Conversely, simpler models, such as logistic regression, provide faster results with adequate accuracy for specific applications [144].

Choosing the right model depends on the clinical context. For situations requiring rapid feedback, simpler models are often preferred, while complex models may be needed for more intricate data patterns. Ultimately, effective AI in RT must ensure both accuracy and computational efficiency, allowing clinicians to make timely decisions without compromising predictive power [166].

However, the implementation of these technologies requires interdisciplinary collaboration between oncologists, radiologists, computer engineers, and bioinformaticians. Furthermore, it is crucial to address the ethical and legal challenges associated with AI in medicine, such as the protection of patient data and the transparency of algorithms [167,168].

5. Conclusions

A precise understanding of dosimetric parameters and their toxicity correlations is essential for optimizing RT plans. This review underscores the importance of parameters like the DVH, Dmax, and Dmean, which are pivotal for predicting toxicity and tailoring

treatments to PCa. Improved toxicity prediction enhances treatment efficacy and minimizes side effects, benefiting patients' QoL.

Emerging technologies, particularly AI and ML, are expected to revolutionize toxicity prediction by analyzing extensive dosimetric and clinical data to identify complex patterns. The integration of advanced techniques such as IGRT and IMRT with AI offers a promising path towards more personalized and effective RT.

The absence of public datasets in current studies underscores a significant need for standardized, large-scale datasets in the field. Standardization across datasets, including common protocols for data collection and uniformity in clinical annotations, would enhance the generalizability and reproducibility of research findings, making it easier to draw reliable conclusions across studies. This would also enable researchers to test and validate models on diverse patient populations, which is critical for ensuring model robustness, especially in personalized RT planning where individual differences greatly impact treatment outcomes.

Large-scale, standardized datasets also facilitate the development of more accurate and unbiased AI models by reducing overfitting and ensuring that models are not tailored to a specific dataset, making them more adaptable to new, unseen data. The availability of such datasets could also accelerate research in the field, as researchers would spend less time gathering and cleaning data and more time on actual model development and validation.

This improvement could greatly benefit future research efforts, fostering collaboration across institutions by providing a common data foundation. Furthermore, open access to standardized data supports transparency and trust, allowing for peer review, which is essential for advancing AI credibility and utility in clinical settings. The creation of standardized datasets would not only enhance research quality but could also speed up the translation of AI-based models into real-world clinical practice.

Future research should address gaps in data and explore innovative applications of AI in various RT modalities, aiming to further refine treatment strategies and optimize patient outcomes while navigating ethical and technical challenges.

Author Contributions: Conceptualization, A.P. and A.C.; methodology, A.P. and A.C.; investigation, A.P., R.C., V.B., M.A. and A.C.; writing—original draft preparation, A.P.; writing—review and editing, A.P., R.C., V.B., M.A., R.L., P.A., G.S. and A.C.; visualization, A.P., R.C. V.B., M.A., R.L., P.A., A.D., D.C., L.B., G.S., D.D.R., A.T. and A.C.; supervision, V.B., M.A., R.C., D.D.R., A.T. and A.C.; project administration, A.C.; funding acquisition, A.C. and P.A. All authors have read and agreed to the published version of the manuscript.

Funding: This work was partially supported by the following projects: "RADIATIONS"—under the PNRR—Next Generation EU, Mission 4, Component 2—Investment 1.5—Cascading Call—Ecosystem of Innovation "THE—Tuscany Health Ecosystem"—code ECS00000017—CUP B83C22003930001, to Albert Comelli; "INNOVA"—Advanced Diagnostic, Project promoted by Italian Ministry of Health—PNC-E3-2022-23681266 PNCHTS-DA 1, CUP D73C22OO2090001, to Viviana Benfante and Pierpaolo Alongi.

Acknowledgments: R.C. is a member of the "Gruppo Nazionale per l'Analisi Matematica, la Probabilità e le loro Applicazioni" (GNAMPA-INdAM).

Conflicts of Interest: The authors declare no conflicts of interest.

Abbreviations

AI	Artificial intelligence
AUC	Area Under the ROC Curve
BT	Brachytherapy
CTCAE	Common Terminology Criteria for Adverse Events

DOI	Digital Object Identifier
GI	Gastrointestinal
GU	Genitourinary
Gy	Gray
ML	Machine learning
PCa	Prostate cancer
RT	Radiotherapy
SBRT	Stereotactic Body Radiotherapy

References

1. Culp, M.B.; Soerjomataram, I.; Efstathiou, J.A.; Bray, F.; Jemal, A. Recent Global Patterns in Prostate Cancer Incidence and Mortality Rates. *Eur. Urol.* **2020**, *77*, 38–52. [CrossRef]
2. Ahdoot, M.; Wilbur, A.R.; Reese, S.E.; Lebastchi, A.H.; Mehralivand, S.; Gomella, P.T.; Bloom, J.; Gurram, S.; Siddiqui, M.; Pinsky, P.; et al. MRI-Targeted, Systematic, and Combined Biopsy for Prostate Cancer Diagnosis. *N. Engl. J. Med.* **2020**, *382*, 917–928. [CrossRef]
3. Teo, M.Y.; Rathkopf, D.E.; Kantoff, P. Treatment of Advanced Prostate Cancer. *Annu. Rev. Med.* **2019**, *70*, 479–499. [CrossRef]
4. Ferrera, G.; D'Alessandro, S.; Cuccia, F.; Serretta, V.; Trapani, G.; Savoca, G.; Mortellaro, G.; Lo Casto, A. Post-operative hypofractionated radiotherapy for prostate cancer: A mono-institutional analysis of toxicity and clinical outcomes. *J. Cancer Res. Clin. Oncol.* **2022**, *148*, 89–95. [CrossRef]
5. Cuccia, F.; Mortellaro, G.; Serretta, V.; Valenti, V.; Tripoli, A.; Gueci, M.; Luca, N.; Lo Casto, A.; Ferrera, G. Hypofractionated postoperative helical tomotherapy in prostate cancer: A mono-institutional report of toxicity and clinical outcomes. *Cancer Manag. Res.* **2018**, *10*, 5053–5060. [CrossRef]
6. Cuccia, F.; Mazzola, R.; Arcangeli, S.; Mortellaro, G.; Figlia, V.; Caminiti, G.; Di Paola, G.; Spera, A.; Iacoviello, G.; Alongi, F.; et al. Moderate hypofractionated helical tomotherapy for localized prostate cancer: Preliminary report of an observational prospective study. *Tumori* **2019**, *105*, 516–523. [CrossRef]
7. Ali, M.; Benfante, V.; Di Raimondo, D.; Salvaggio, G.; Tuttolomondo, A.; Comelli, A. Recent Developments in Nanoparticle Formulations for Resveratrol Encapsulation as an Anticancer Agent. *Pharmaceuticals* **2024**, *17*, 126. [CrossRef]
8. Ali, M.; Benfante, V.; Di Raimondo, D.; Laudicella, R.; Tuttolomondo, A.; Comelli, A. A Review of Advances in Molecular Imaging of Rheumatoid Arthritis: From In Vitro to Clinic Applications Using Radiolabeled Targeting Vectors with Technetium-99m. *Life* **2024**, *14*, 751. [CrossRef]
9. Podder, T.K.; Fredman, E.T.; Ellis, R.J. Advances in Radiotherapy for Prostate Cancer Treatment. *Adv. Exp. Med. Biol.* **2018**, *1096*, 31–47. [CrossRef] [PubMed]
10. Wallis, C.J.D.; Saskin, R.; Choo, R.; Herschorn, S.; Kodama, R.T.; Satkunasivam, R.; Shah, P.S.; Danjoux, C.; Nam, R.K. Surgery Versus Radiotherapy for Clinically-localized Prostate Cancer: A Systematic Review and Meta-analysis. *Eur. Urol.* **2016**, *70*, 21–30. [CrossRef] [PubMed]
11. Schick, U.; Latorzeff, I.; Sargos, P. Postoperative radiotherapy in prostate cancer: Dose and volumes. *Cancer Radiother.* **2021**, *25*, 674–678. [CrossRef] [PubMed]
12. Reijnen, C.; Brunenberg, E.J.L.; Kerkmeijer, L.G.W. Advancing the treatment of localized prostate cancer with MR-guided radiotherapy. *Prostate Cancer Prostatic Dis.* **2023**, *26*, 50–52. [CrossRef] [PubMed]
13. Hamdy, F.C.; Donovan, J.L.; Lane, J.A.; Metcalfe, C.; Davis, M.; Turner, E.L.; Martin, R.M.; Young, G.J.; Walsh, E.I.; Bryant, R.J.; et al. Fifteen-Year Outcomes after Monitoring, Surgery, or Radiotherapy for Prostate Cancer. *N. Engl. J. Med.* **2023**, *388*, 1547–1558. [CrossRef] [PubMed]
14. James, N.D.; Tannock, I.; N'Dow, J.; Feng, F.; Gillessen, S.; Ali, S.A.; Trujillo, B.; Al-Lazikani, B.; Attard, G.; Bray, F.; et al. The Lancet Commission on prostate cancer: Planning for the surge in cases. *Lancet* **2024**, *403*, 1683–1722. [CrossRef]
15. Ali, M.; Benfante, V.; Stefano, A.; Yezzi, A.; Di Raimondo, D.; Tuttolomondo, A.; Comelli, A. Anti-Arthritic and Anti-Cancer Activities of Polyphenols: A Review of the Most Recent In Vitro Assays. *Life* **2023**, *13*, 361. [CrossRef]
16. Benfante, V.; Stefano, A.; Ali, M.; Laudicella, R.; Arancio, W.; Cucchiara, A.; Caruso, F.; Cammarata, F.P.; Coronnello, C.; Russo, G.; et al. An Overview of In Vitro Assays of 64Cu-, 68Ga-, 125I-, and 99mTc-Labelled Radiopharmaceuticals Using Radiometric Counters in the Era of Radiotheranostics. *Diagnostics* **2023**, *13*, 1210. [CrossRef]
17. Cairone, L.; Benfante, V.; Bignardi, S.; Marinozzi, F.; Yezzi, A.; Tuttolomondo, A.; Salvaggio, G.; Bini, F.; Comelli, A. Robustness of Radiomics Features to Varying Segmentation Algorithms in Magnetic Resonance Images. In Proceedings of the Image Analysis and Processing, ICIAP 2022 Workshops: ICIAP International Workshops, Lecce, Italy, 23–27 May 2022; Revised Selected Papers, Part I. Springer: Berlin/Heidelberg, Germany, 2022; pp. 462–472.
18. Jaffray, D.A.; Gospodarowicz, M.K. Radiation Therapy for Cancer. In *Cancer: Disease Control Priorities*, 3rd ed.; Gelband, H., Jha, P., Sankaranarayanan, R., Horton, S., Eds.; The International Bank for Reconstruction and Development/The World Bank: Washington, DC, USA, 2015; Volume 3, ISBN 978-1-4648-0349-9.
19. Miller, K.D.; Nogueira, L.; Devasia, T.; Mariotto, A.B.; Yabroff, K.R.; Jemal, A.; Kramer, J.; Siegel, R.L. Cancer treatment and survivorship statistics, 2022. *CA Cancer J. Clin.* **2022**, *72*, 409–436. [CrossRef]

20. DeSantis, C.E.; Miller, K.D.; Dale, W.; Mohile, S.G.; Cohen, H.J.; Leach, C.R.; Goding Sauer, A.; Jemal, A.; Siegel, R.L. Cancer statistics for adults aged 85 years and older, 2019. *CA Cancer J. Clin.* **2019**, *69*, 452–467. [CrossRef]
21. Siegel, R.L.; Miller, K.D.; Fuchs, H.E.; Jemal, A. Cancer Statistics, 2021. *CA Cancer J. Clin.* **2021**, *71*, 7–33. [CrossRef]
22. Majeed, H.; Gupta, V. Adverse Effects of Radiation Therapy. In *StatPearls*; StatPearls Publishing: Treasure Island, FL, USA, 2024.
23. Wang, K.; Tepper, J.E. Radiation therapy-associated toxicity: Etiology, management, and prevention. *CA Cancer J. Clin.* **2021**, *71*, 437–454. [CrossRef]
24. Rancati, T.; Palorini, F.; Cozzarini, C.; Fiorino, C.; Valdagni, R. Understanding urinary toxicity after radiotherapy for prostate cancer: First steps forward. *Tumori* **2017**, *103*, 395–404. [CrossRef] [PubMed]
25. Vinciguerra, A.; Augurio, A.; Rosa, C.; Fasciolo, D.; Borgia, M.; Milone, V.; Marchioni, M.; DI Nicola, M.; Genovesi, D.; Caravatta, L. Lower Bladder Toxicity of Salvage Versus Adjuvant Modern Radiotherapy for Prostate Cancer Patients. *In Vivo* **2022**, *36*, 1375–1382. [CrossRef] [PubMed]
26. Armstrong, N.; Bahl, A.; Pinkawa, M.; Ryder, S.; Ahmadu, C.; Ross, J.; Bhattacharyya, S.; Woodward, E.; Battaglia, S.; Binns, J.; et al. SpaceOAR Hydrogel Spacer for Reducing Radiation Toxicity During Radiotherapy for Prostate Cancer. A Systematic Review. *Urology* **2021**, *156*, e74–e85. [CrossRef] [PubMed]
27. Groen, V.H.; Zuithoff, N.P.A.; van Schie, M.; Monninkhof, E.M.; Kunze-Busch, M.; de Boer, H.C.J.; van der Voort van Zyp, J.; Pos, F.J.; Smeenk, R.J.; Haustermans, K.; et al. Anorectal dose-effect relations for late gastrointestinal toxicity following external beam radiotherapy for prostate cancer in the FLAME trial. *Radiother. Oncol.* **2021**, *162*, 98–104. [CrossRef] [PubMed]
28. Song, J.; Corkum, M.T.; Loblaw, D.A.; Chung, H.T.; Tseng, C.L.; Cheung, P.; Szumacher, E.; Liu, S.K.; Chu, W.; Davidson, M.T.M.; et al. Dosimetric Parameters Predictive of Treatment-Related Toxicity in High Dose-Rate Brachytherapy as Monotherapy for Prostate Cancer. *Int. J. Radiat. Oncol. Biol. Phys.* **2023**, *117*, e438–e439. [CrossRef]
29. Yue, H.; Li, X.; You, J.; Feng, P.; Du, Y.; Wang, R.; Wu, H.; Cheng, J.; Ding, K.; Jing, B. Acute hematologic toxicity prediction using dosimetric and radiomics features in patients with cervical cancer: Does the treatment regimen matter? *Front. Oncol.* **2024**, *14*, 1365897. [CrossRef]
30. Pasquier, D.; Bataille, B.; Le Tinier, F.; Bennadji, R.; Langin, H.; Escande, A.; Tresch, E.; Darloy, F.; Carlier, D.; Crop, F.; et al. Correlation between toxicity and dosimetric parameters for adjuvant intensity modulated radiation therapy of breast cancer: A prospective study. *Sci. Rep.* **2021**, *11*, 3626. [CrossRef]
31. Qi, X.S.; Wang, J.P.; Gomez, C.L.; Shao, W.; Xu, X.; King, C.; Low, D.A.; Steinberg, M.; Kupelian, P. Plan quality and dosimetric association of patient-reported rectal and urinary toxicities for prostate stereotactic body radiotherapy. *Radiother. Oncol.* **2016**, *121*, 113–117. [CrossRef]
32. Ito, Y.; Igawa, S.; Ohishi, Y.; Uehara, J.; Yamamoto, A.I.; Iizuka, H. Prognostic indicators in 35 patients with extramammary Paget's disease. *Dermatol. Surg.* **2012**, *38*, 1938–1944. [CrossRef]
33. Dipasquale, G.; Zilli, T.; Fiorino, C.; Achard, V.; Rouzaud, M.; Miralbell, R. Urinary toxicity after salvage re-irradiation for prostate cancer local failure after definitive radiotherapy: A clinical and dosimetric prognostic factors analysis. *J. Contemp. Brachytherapy* **2022**, *14*, 222–226. [CrossRef]
34. Alayed, Y.; Davidson, M.; Quon, H.; Cheung, P.; Chu, W.; Chung, H.T.; Vesprini, D.; Ong, A.; Chowdhury, A.; Liu, S.K.; et al. Dosimetric predictors of toxicity and quality of life following prostate stereotactic ablative radiotherapy. *Radiother. Oncol.* **2020**, *144*, 135–140. [CrossRef] [PubMed]
35. Kougioumtzopoulou, A.; Syrigos, N.; Zygogianni, A.; Georgakopoulos, I.; Platoni, K.; Patatoukas, G.; Tzannis, K.; Bamias, A.; Kelekis, N.; Kouloulias, V. Comprehensive 3DCRT Hypofractionated Radiotherapy Schedule for Localized Prostate Adenocarcinoma in the Era of IMRT: Dosimetric and Endoscopic Analysis. *Cancers* **2024**, *16*, 1192. [CrossRef] [PubMed]
36. Sanfratello, A.; Cusumano, D.; Piras, A.; Boldrini, L.; D'Aviero, A.; Fricano, P.; Messina, M.; Vaglica, M.; Galanti, D.; Spada, M.; et al. New dosimetric parameters to predict ano-rectal toxicity during radiotherapy treatment. *Phys. Med.* **2022**, *99*, 55–60. [CrossRef] [PubMed]
37. Giaccone, P.; Benfante, V.; Stefano, A.; Cammarata, F.P.; Russo, G.; Comelli, A. PET Images Atlas-Based Segmentation Performed in Native and in Template Space: A Radiomics Repeatability Study in Mouse Models. In Proceedings of the Image Analysis and Processing, ICIAP 2022 Workshops: ICIAP International Workshops, Lecce, Italy, 23–27 May 2022; Revised Selected Papers, Part I. Springer: Berlin/Heidelberg, Germany, 2022; pp. 351–361.
38. Mann, M.; Kumar, C.; Zeng, W.-F.; Strauss, M.T. Artificial intelligence for proteomics and biomarker discovery. *Cell Syst.* **2021**, *12*, 759–770. [CrossRef] [PubMed]
39. Santos, Á.O.D.; da Silva, E.S.; Couto, L.M.; Reis, G.V.L.; Belo, V.S. The use of artificial intelligence for automating or semi-automating biomedical literature analyses: A scoping review. *J. Biomed. Inform.* **2023**, *142*, 104389. [CrossRef]
40. Azadi Moghadam, P.; Bashashati, A.; Goldenberg, S.L. Artificial Intelligence and Pathomics: Prostate Cancer. *Urol. Clin. N. Am.* **2024**, *51*, 15–26. [CrossRef]
41. Ferraro, D.A.; Lehner, F.; Becker, A.S.; Kranzbühler, B.; Kudura, K.; Mebert, I.; Messerli, M.; Hermanns, T.; Eberli, D.; Burger, I.A. Improved oncological outcome after radical prostatectomy in patients staged with 68Ga-PSMA-11 PET: A single-center retrospective cohort comparison. *Eur. J. Nucl. Med. Mol. Imaging* **2021**, *48*, 1219–1228. [CrossRef]
42. Agnello, L.; Comelli, A.; Ardizzone, E.; Vitabile, S. Unsupervised tissue classification of brain MR images for voxel-based morphometry analysis. *Int. J. Imaging Syst. Technol.* **2016**, *26*, 136–150. [CrossRef]

43. Wang, B.; Lei, Y.; Tian, S.; Wang, T.; Liu, Y.; Patel, P.; Jani, A.B.; Mao, H.; Curran, W.J.; Liu, T.; et al. Deeply supervised 3D fully convolutional networks with group dilated convolution for automatic MRI prostate segmentation. *Med. Phys.* **2019**, *46*, 1707–1718. [CrossRef]
44. Zhao, X.; Wu, Y.; Song, G.; Li, Z.; Zhang, Y.; Fan, Y. A deep learning model integrating FCNNs and CRFs for brain tumor segmentation. *Med. Image Anal.* **2018**, *43*, 98–111. [CrossRef]
45. Corso, R.; Comelli, A.; Salvaggio, G.; Tegolo, D. New Parametric 2D Curves for Modeling Prostate Shape in Magnetic Resonance Images. *Symmetry* **2024**, *16*, 755. [CrossRef]
46. Fan, D.-P.; Zhou, T.; Ji, G.-P.; Zhou, Y.; Chen, G.; Fu, H.; Shen, J.; Shao, L. Inf-Net: Automatic COVID-19 Lung Infection Segmentation From CT Images. *IEEE Trans. Med. Imaging* **2020**, *39*, 2626–2637. [CrossRef] [PubMed]
47. Cha, E.; Elguindi, S.; Onochie, I.; Gorovets, D.; Deasy, J.O.; Zelefsky, M.; Gillespie, E.F. Clinical implementation of deep learning contour autosegmentation for prostate radiotherapy. *Radiother. Oncol.* **2021**, *159*, 1–7. [CrossRef] [PubMed]
48. De Kerf, G.; Claessens, M.; Raouassi, F.; Mercier, C.; Stas, D.; Ost, P.; Dirix, P.; Verellen, D. A geometry and dose-volume based performance monitoring of artificial intelligence models in radiotherapy treatment planning for prostate cancer. *Phys. Imaging Radiat. Oncol.* **2023**, *28*, 100494. [CrossRef]
49. Doolan, P.J.; Charalambous, S.; Roussakis, Y.; Leczynski, A.; Peratikou, M.; Benjamin, M.; Ferentinos, K.; Strouthos, I.; Zamboglou, C.; Karagiannis, E. A clinical evaluation of the performance of five commercial artificial intelligence contouring systems for radiotherapy. *Front. Oncol.* **2023**, *13*, 1213068. [CrossRef]
50. Zhang, Y.; Liang, Y.; Ding, J.; Amjad, A.; Paulson, E.; Ahunbay, E.; Hall, W.A.; Erickson, B.; Li, X.A. A Prior Knowledge-Guided, Deep Learning-Based Semiautomatic Segmentation for Complex Anatomy on Magnetic Resonance Imaging. *Int. J. Radiat. Oncol. Biol. Phys.* **2022**, *114*, 349–359. [CrossRef]
51. D'Aviero, A.; Re, A.; Catucci, F.; Piccari, D.; Votta, C.; Piro, D.; Piras, A.; Di Dio, C.; Iezzi, M.; Preziosi, F.; et al. Clinical Validation of a Deep-Learning Segmentation Software in Head and Neck: An Early Analysis in a Developing Radiation Oncology Center. *Int. J. Environ. Res. Public Health* **2022**, *19*, 9057. [CrossRef]
52. Radici, L.; Ferrario, S.; Borca, V.C.; Cante, D.; Paolini, M.; Piva, C.; Baratto, L.; Franco, P.; La Porta, M.R. Implementation of a Commercial Deep Learning-Based Auto Segmentation Software in Radiotherapy: Evaluation of Effectiveness and Impact on Workflow. *Life* **2022**, *12*, 2088. [CrossRef]
53. Min, X.; Li, M.; Dong, D.; Feng, Z.; Zhang, P.; Ke, Z.; You, H.; Han, F.; Ma, H.; Tian, J.; et al. Multi-parametric MRI-based radiomics signature for discriminating between clinically significant and insignificant prostate cancer: Cross-validation of a machine learning method. *Eur. J. Radiol.* **2019**, *115*, 16–21. [CrossRef]
54. Hectors, S.J.; Cherny, M.; Yadav, K.K.; Beksaç, A.T.; Thulasidass, H.; Lewis, S.; Davicioni, E.; Wang, P.; Tewari, A.K.; Taouli, B. Radiomics Features Measured with Multiparametric Magnetic Resonance Imaging Predict Prostate Cancer Aggressiveness. *J. Urol.* **2019**, *202*, 498–505. [CrossRef]
55. Lo Casto, A.; Spartivento, G.; Benfante, V.; Di Raimondo, R.; Ali, M.; Di Raimondo, D.; Tuttolomondo, A.; Stefano, A.; Yezzi, A.; Comelli, A. Artificial Intelligence for Classifying the Relationship between Impacted Third Molar and Mandibular Canal on Panoramic Radiographs. *Life* **2023**, *13*, 1441. [CrossRef] [PubMed]
56. Canfora, I.; Cutaia, G.; Marcianò, M.; Calamia, M.; Faraone, R.; Cannella, R.; Benfante, V.; Comelli, A.; Guercio, G.; Giuseppe, L.R.; et al. A Predictive System to Classify Preoperative Grading of Rectal Cancer Using Radiomics Features. In Proceedings of the Image Analysis and Processing, ICIAP 2022 Workshops: ICIAP International Workshops, Lecce, Italy, 23–27 May 2022; Revised Selected Papers, Part I. Springer: Berlin/Heidelberg, Germany, 2022; pp. 431–440.
57. Benfante, V.; Salvaggio, G.; Ali, M.; Cutaia, G.; Salvaggio, L.; Salerno, S.; Busè, G.; Tulone, G.; Pavan, N.; Di Raimondo, D.; et al. Grading and Staging of Bladder Tumors Using Radiomics Analysis in Magnetic Resonance Imaging. In Proceedings of the Image Analysis and Processing—ICIAP 2023 Workshops, Udine, Italy, 11–15 September 2023; Proceedings, Part II. Springer: Berlin/Heidelberg, Germany, 2024; pp. 93–103.
58. Corso, R.; Stefano, A.; Salvaggio, G.; Comelli, A. Shearlet Transform Applied to a Prostate Cancer Radiomics Analysis on MR Images. *Mathematics* **2024**, *12*, 1296. [CrossRef]
59. Ali, M.; Benfante, V.; Cutaia, G.; Salvaggio, L.; Rubino, S.; Portoghese, M.; Ferraro, M.; Corso, R.; Piraino, G.; Ingrassia, T.; et al. Prostate Cancer Detection: Performance of Radiomics Analysis in Multiparametric MRI. In Proceedings of the Image Analysis and Processing—ICIAP 2023 Workshops, Udine, Italy, 11–15 September 2023; Proceedings, Part II. Springer: Berlin/Heidelberg, Germany, 2024; pp. 83–92.
60. Abdollahi, H.; Mofid, B.; Shiri, I.; Razzaghdoust, A.; Saadipoor, A.; Mahdavi, A.; Galandooz, H.M.; Mahdavi, S.R. Machine learning-based radiomic models to predict intensity-modulated radiation therapy response, Gleason score and stage in prostate cancer. *Radiol. Med.* **2019**, *124*, 555–567. [CrossRef]
61. Beesley, L.J.; Morgan, T.M.; Spratt, D.E.; Singhal, U.; Feng, F.Y.; Furgal, A.C.; Jackson, W.C.; Daignault, S.; Taylor, J.M.G. Individual and Population Comparisons of Surgery and Radiotherapy Outcomes in Prostate Cancer Using Bayesian Multistate Models. *JAMA Netw. Open* **2019**, *2*, e187765. [CrossRef] [PubMed]
62. Yahya, N.; Ebert, M.A.; Bulsara, M.; House, M.J.; Kennedy, A.; Joseph, D.J.; Denham, J.W. Statistical-learning strategies generate only modestly performing predictive models for urinary symptoms following external beam radiotherapy of the prostate: A comparison of conventional and machine-learning methods. *Med. Phys.* **2016**, *43*, 2040. [CrossRef] [PubMed]

63. Alongi, P.; Stefano, A.; Comelli, A.; Spataro, A.; Formica, G.; Laudicella, R.; Lanzafame, H.; Panasiti, F.; Longo, C.; Midiri, F.; et al. Artificial Intelligence Applications on Restaging [18F]FDG PET/CT in Metastatic Colorectal Cancer: A Preliminary Report of Morpho-Functional Radiomics Classification for Prediction of Disease Outcome. *Appl. Sci.* **2022**, *12*, 2941. [CrossRef]
64. Russo, G.; Stefano, A.; Alongi, P.; Comelli, A.; Catalfamo, B.; Mantarro, C.; Longo, C.; Altieri, R.; Certo, F.; Cosentino, S.; et al. Feasibility on the Use of Radiomics Features of 11[C]-MET PET/CT in Central Nervous System Tumours: Preliminary Results on Potential Grading Discrimination Using a Machine Learning Model. *Curr. Oncol.* **2021**, *28*, 5318–5331. [CrossRef]
65. Pavone, A.M.; Benfante, V.; Giaccone, P.; Stefano, A.; Torrisi, F.; Russo, V.; Serafini, D.; Richiusa, S.; Pometti, M.; Scopelliti, F.; et al. Biodistribution Assessment of a Novel 68Ga-Labeled Radiopharmaceutical in a Cancer Overexpressing CCK2R Mouse Model: Conventional and Radiomics Methods for Analysis. *Life* **2024**, *14*, 409. [CrossRef]
66. Pomykala, K.L.; Hadaschik, B.A.; Sartor, O.; Gillessen, S.; Sweeney, C.J.; Maughan, T.; Hofman, M.S.; Herrmann, K. Next generation radiotheranostics promoting precision medicine. *Ann. Oncol.* **2023**, *34*, 507–519. [CrossRef]
67. Benfante, V.; Stefano, A.; Comelli, A.; Giaccone, P.; Cammarata, F.P.; Richiusa, S.; Scopelliti, F.; Pometti, M.; Ficarra, M.; Cosentino, S.; et al. A New Preclinical Decision Support System Based on PET Radiomics: A Preliminary Study on the Evaluation of an Innovative 64Cu-Labeled Chelator in Mouse Models. *J. Imaging* **2022**, *8*, 92. [CrossRef]
68. Bauckneht, M.; Ciccarese, C.; Laudicella, R.; Mosillo, C.; D'Amico, F.; Anghelone, A.; Strusi, A.; Beccia, V.; Bracarda, S.; Fornarini, G.; et al. Theranostics revolution in prostate cancer: Basics, clinical applications, open issues and future perspectives. *Cancer Treat. Rev.* **2024**, *124*, 102698. [CrossRef] [PubMed]
69. Rupp, N.J.; Freiberger, S.N.; Ferraro, D.A.; Laudicella, R.; Heimer, J.; Muehlematter, U.J.; Poyet, C.; Moch, H.; Eberli, D.; Rüschoff, J.H.; et al. Immunohistochemical ERG positivity is associated with decreased PSMA expression and lower visibility in corresponding [68Ga]Ga-PSMA-11 PET scans of primary prostate cancer. *Eur. J. Nucl. Med. Mol. Imaging* **2024**. *ahead of print*. [CrossRef] [PubMed]
70. Laudicella, R.; Comelli, A.; Liberini, V.; Vento, A.; Stefano, A.; Spataro, A.; Crocè, L.; Baldari, S.; Bambaci, M.; Deandreis, D.; et al. [68Ga]DOTATOC PET/CT Radiomics to Predict the Response in GEP-NETs Undergoing [177Lu]DOTATOC PRRT: The "Theragnomics" Concept. *Cancers* **2022**, *14*, 984. [CrossRef] [PubMed]
71. Kawamura, M.; Kamomae, T.; Yanagawa, M.; Kamagata, K.; Fujita, S.; Ueda, D.; Matsui, Y.; Fushimi, Y.; Fujioka, T.; Nozaki, T.; et al. Revolutionizing radiation therapy: The role of AI in clinical practice. *J. Radiat. Res.* **2024**, *65*, 1–9. [CrossRef] [PubMed]
72. Georgiou, M.F.; Nielsen, J.A.; Chiriboga, R.; Kuker, R.A. An Artificial Intelligence System for Optimizing Radioactive Iodine Therapy Dosimetry. *J. Clin. Med.* **2023**, *13*, 117. [CrossRef]
73. Giraud, P.; Bibault, J.-E. Artificial intelligence in radiotherapy: Current applications and future trends. In *Diagnostic and Interventional Imaging*; Elsevier: Amsterdam, The Netherlands, 2024. [CrossRef]
74. Siddique, S.; Chow, J.C.L. Artificial intelligence in radiotherapy. *Rep. Pract. Oncol. Radiother.* **2020**, *25*, 656–666. [CrossRef]
75. Isaksson, L.J.; Pepa, M.; Zaffaroni, M.; Marvaso, G.; Alterio, D.; Volpe, S.; Corrao, G.; Augugliaro, M.; Starzyńska, A.; Leonardi, M.C.; et al. Machine Learning-Based Models for Prediction of Toxicity Outcomes in Radiotherapy. *Front. Oncol.* **2020**, *10*, 790. [CrossRef]
76. Krishnamurthy, R.; Mummudi, N.; Goda, J.S.; Chopra, S.; Heijmen, B.; Swamidas, J. Using Artificial Intelligence for Optimization of the Processes and Resource Utilization in Radiotherapy. *JCO Glob. Oncol.* **2022**, *8*, e2100393. [CrossRef]
77. Cusumano, D.; Boldrini, L.; Yadav, P.; Casà, C.; Lee, S.L.; Romano, A.; Piras, A.; Chiloiro, G.; Placidi, L.; Catucci, F.; et al. Delta Radiomics Analysis for Local Control Prediction in Pancreatic Cancer Patients Treated Using Magnetic Resonance Guided Radiotherapy. *Diagnostics* **2021**, *11*, 72. [CrossRef]
78. Cusumano, D.; Boldrini, L.; Yadav, P.; Yu, G.; Musurunu, B.; Chiloiro, G.; Piras, A.; Lenkowicz, J.; Placidi, L.; Broggi, S.; et al. External Validation of Early Regression Index (ERITCP) as Predictor of Pathologic Complete Response in Rectal Cancer Using Magnetic Resonance-Guided Radiation Therapy. *Int. J. Radiat. Oncol. Biol. Phys.* **2020**, *108*, 1347–1356. [CrossRef]
79. Boldrini, L.; D'Aviero, A.; De Felice, F.; Desideri, I.; Grassi, R.; Greco, C.; Iorio, G.C.; Nardone, V.; Piras, A.; Salvestrini, V. Artificial intelligence applied to image-guided radiation therapy (IGRT): A systematic review by the Young Group of the Italian Association of Radiotherapy and Clinical Oncology (yAIRO). *Radiol. Med.* **2023**, *129*, 133–151. [CrossRef]
80. De Ruysscher, D.; Niedermann, G.; Burnet, N.G.; Siva, S.; Lee, A.W.M.; Hegi-Johnson, F. Radiotherapy toxicity. *Nat. Rev. Dis. Primers* **2019**, *5*, 13. [CrossRef]
81. Lardas, M.; Liew, M.; van den Bergh, R.C.; De Santis, M.; Bellmunt, J.; Van den Broeck, T.; Cornford, P.; Cumberbatch, M.G.; Fossati, N.; Gross, T.; et al. Quality of Life Outcomes after Primary Treatment for Clinically Localised Prostate Cancer: A Systematic Review. *Eur. Urol.* **2017**, *72*, 869–885. [CrossRef]
82. Ma, T.M.; Ballas, L.K.; Wilhalme, H.; Sachdeva, A.; Chong, N.; Sharma, S.; Yang, T.; Basehart, V.; Reiter, R.E.; Saigal, C.; et al. Quality-of-Life Outcomes and Toxicity Profile Among Patients With Localized Prostate Cancer After Radical Prostatectomy Treated With Stereotactic Body Radiation: The SCIMITAR Multicenter Phase 2 Trial. *Int. J. Radiat. Oncol. Biol. Phys.* **2023**, *115*, 142–152. [CrossRef]
83. Poźniak-Balicka, R.; Chomiak, B.; Wośkowiak, P.; Nowicki, N.; Bojarski, J.; Salagierski, M. Does the radiation approach affect acute toxicity in prostate cancer patients? A comparison of four radiation techniques. *Cent. Eur. J. Urol.* **2020**, *73*, 295–299. [CrossRef]
84. Sinzabakira, F.; Brand, V.; Heemsbergen, W.D.; Incrocci, L. Acute and late toxicity patterns of moderate hypo-fractionated radiotherapy for prostate cancer: A systematic review and meta-analysis. *Clin. Transl. Radiat. Oncol.* **2023**, *40*, 100612. [CrossRef] [PubMed]

85. Brand, D.H.; Tree, A.C.; Ostler, P.; van der Voet, H.; Loblaw, A.; Chu, W.; Ford, D.; Tolan, S.; Jain, S.; Martin, A.; et al. Intensity-modulated fractionated radiotherapy versus stereotactic body radiotherapy for prostate cancer (PACE-B): Acute toxicity findings from an international, randomised, open-label, phase 3, non-inferiority trial. *Lancet Oncol.* **2019**, *20*, 1531–1543. [CrossRef] [PubMed]
86. Gill, S.; Thomas, J.; Fox, C.; Kron, T.; Rolfo, A.; Leahy, M.; Chander, S.; Williams, S.; Tai, K.H.; Duchesne, G.M.; et al. Acute toxicity in prostate cancer patients treated with and without image-guided radiotherapy. *Radiat. Oncol.* **2011**, *6*, 145. [CrossRef] [PubMed]
87. Ohri, N.; Dicker, A.P.; Showalter, T.N. Late toxicity rates following definitive radiotherapy for prostate cancer. *Can. J. Urol.* **2012**, *19*, 6373–6380. [PubMed]
88. Alexander, A.; Gagne, I.; Bahl, G.; Kim, D.; Mestrovic, A.; Ye, A.; Kwan, W. Late Toxicity of Prostate Ultrahypofractionated Radiation Therapy Compared With Moderate Hypofractionation in a Randomized Trial. *Int. J. Radiat. Oncol. Biol. Phys.* **2024**, *119*, 110–118. [CrossRef]
89. David, R.; Buckby, A.; Kahokehr, A.A.; Lee, J.; Watson, D.I.; Leung, J.; O'Callaghan, M.E. Long term genitourinary toxicity following curative intent intensity-modulated radiotherapy for prostate cancer: A systematic review and meta-analysis. *Prostate Cancer Prostatic Dis.* **2023**, *26*, 8–15. [CrossRef] [PubMed]
90. Nasser, N.J.; Klein, J.; Agbarya, A. Markers of Toxicity and Response to Radiation Therapy in Patients With Prostate Cancer. *Adv. Radiat. Oncol.* **2021**, *6*, 100603. [CrossRef] [PubMed]
91. Wang, K.; Mavroidis, P.; Royce, T.J.; Falchook, A.D.; Collins, S.P.; Sapareto, S.; Sheets, N.C.; Fuller, D.B.; El Naqa, I.; Yorke, E.; et al. Prostate Stereotactic Body Radiation Therapy: An Overview of Toxicity and Dose Response. *Int. J. Radiat. Oncol. Biol. Phys.* **2021**, *110*, 237–248. [CrossRef] [PubMed]
92. Henríquez-Hernández, L.A.; Bordón, E.; Pinar, B.; Lloret, M.; Rodríguez-Gallego, C.; Lara, P.C. Prediction of normal tissue toxicity as part of the individualized treatment with radiotherapy in oncology patients. *Surg. Oncol.* **2012**, *21*, 201–206. [CrossRef] [PubMed]
93. D'Avino, V.; Palma, G.; Liuzzi, R.; Conson, M.; Doria, F.; Salvatore, M.; Pacelli, R.; Cella, L. Prediction of gastrointestinal toxicity after external beam radiotherapy for localized prostate cancer. *Radiat. Oncol.* **2015**, *10*, 80. [CrossRef]
94. Hostova, B.; Matula, P.; Dubinsky, P. Prediction of toxicities of prostate cancer radiotherapy. *Neoplasma* **2016**, *63*, 163–168. [CrossRef]
95. Tătaru, O.S.; Vartolomei, M.D.; Rassweiler, J.J.; Virgil, O.; Lucarelli, G.; Porpiglia, F.; Amparore, D.; Manfredi, M.; Carrieri, G.; Falagario, U.; et al. Artificial Intelligence and Machine Learning in Prostate Cancer Patient Management-Current Trends and Future Perspectives. *Diagnostics* **2021**, *11*, 354. [CrossRef]
96. Hassan, J.; Saeed, S.M.; Deka, L.; Uddin, M.J.; Das, D.B. Applications of Machine Learning (ML) and Mathematical Modeling (MM) in Healthcare with Special Focus on Cancer Prognosis and Anticancer Therapy: Current Status and Challenges. *Pharmaceutics* **2024**, *16*, 260. [CrossRef]
97. Baydoun, A.; Jia, A.Y.; Zaorsky, N.G.; Kashani, R.; Rao, S.; Shoag, J.E.; Vince, R.A.; Bittencourt, L.K.; Zuhour, R.; Price, A.T.; et al. Artificial intelligence applications in prostate cancer. *Prostate Cancer Prostatic Dis.* **2024**, *27*, 37–45. [CrossRef]
98. Howard, F.M.; Kochanny, S.; Koshy, M.; Spiotto, M.; Pearson, A.T. Machine Learning-Guided Adjuvant Treatment of Head and Neck Cancer. *JAMA Netw. Open* **2020**, *3*, e2025881. [CrossRef]
99. Avanzo, M.; Stancanello, J.; Pirrone, G.; Sartor, G. Radiomics and deep learning in lung cancer. *Strahlenther. Onkol.* **2020**, *196*, 879–887. [CrossRef] [PubMed]
100. Deist, T.M.; Dankers, F.J.W.M.; Valdes, G.; Wijsman, R.; Hsu, I.-C.; Oberije, C.; Lustberg, T.; van Soest, J.; Hoebers, F.; Jochems, A.; et al. Machine learning algorithms for outcome prediction in (chemo)radiotherapy: An empirical comparison of classifiers. *Med. Phys.* **2018**, *45*, 3449–3459. [CrossRef] [PubMed]
101. Yang, Z.; Olszewski, D.; He, C.; Pintea, G.; Lian, J.; Chou, T.; Chen, R.C.; Shtylla, B. Machine learning and statistical prediction of patient quality-of-life after prostate radiation therapy. *Comput. Biol. Med.* **2021**, *129*, 104127. [CrossRef] [PubMed]
102. Page, M.J.; McKenzie, J.E.; Bossuyt, P.M.; Boutron, I.; Hoffmann, T.C.; Mulrow, C.D.; Shamseer, L.; Tetzlaff, J.M.; Akl, E.A.; Brennan, S.E.; et al. The PRISMA 2020 statement: An updated guideline for reporting systematic reviews. *BMJ* **2021**, *372*, n71. [CrossRef] [PubMed]
103. Fiorino, C.; Cozzarini, C.; Vavassori, V.; Sanguineti, G.; Bianchi, C.; Cattaneo, G.M.; Foppiano, F.; Magli, A.; Piazzolla, A. Relationships between DVHs and late rectal bleeding after radiotherapy for prostate cancer: Analysis of a large group of patients pooled from three institutions. *Radiother. Oncol.* **2002**, *64*, 1–12. [CrossRef]
104. Cozzarini, C.; Fiorino, C.; Ceresoli, G.L.; Cattaneo, G.M.; Bolognesi, A.; Calandrino, R.; Villa, E. Significant correlation between rectal DVH and late bleeding in patients treated after radical prostatectomy with conformal or conventional radiotherapy (66.6-70.2 Gy). *Int. J. Radiat. Oncol. Biol. Phys.* **2003**, *55*, 688–694. [CrossRef]
105. Fiorino, C.; Sanguineti, G.; Cozzarini, C.; Fellin, G.; Foppiano, F.; Menegotti, L.; Piazzolla, A.; Vavassori, V.; Valdagni, R. Rectal dose-volume constraints in high-dose radiotherapy of localized prostate cancer. *Int. J. Radiat. Oncol. Biol. Phys.* **2003**, *57*, 953–962. [CrossRef]
106. Zapatero, A.; García-Vicente, F.; Modolell, I.; Alcántara, P.; Floriano, A.; Cruz-Conde, A.; Torres, J.J.; Pérez-Torrubia, A. Impact of mean rectal dose on late rectal bleeding after conformal radiotherapy for prostate cancer: Dose-volume effect. *Int. J. Radiat. Oncol. Biol. Phys.* **2004**, *59*, 1343–1351. [CrossRef]

107. Fiorino, C.; Fellin, G.; Rancati, T.; Vavassori, V.; Bianchi, C.; Borca, V.C.; Girelli, G.; Mapelli, M.; Menegotti, L.; Nava, S.; et al. Clinical and dosimetric predictors of late rectal syndrome after 3D-CRT for localized prostate cancer: Preliminary results of a multicenter prospective study. *Int. J. Radiat. Oncol. Biol. Phys.* **2008**, *70*, 1130–1137. [CrossRef]
108. Arcangeli, S.; Strigari, L.; Soete, G.; De Meerleer, G.; Gomellini, S.; Fonteyne, V.; Storme, G.; Arcangeli, G. Clinical and dosimetric predictors of acute toxicity after a 4-week hypofractionated external beam radiotherapy regimen for prostate cancer: Results from a multicentric prospective trial. *Int. J. Radiat. Oncol. Biol. Phys.* **2009**, *73*, 39–45. [CrossRef]
109. Faria, S.; Joshua, B.; Patrocinio, H.; Dal Pra, A.; Cury, F.; Velly, A.M.; Souhami, L. Searching for optimal dose-volume constraints to reduce rectal toxicity after hypofractionated radiotherapy for prostate cancer. *Clin. Oncol.* **2010**, *22*, 810–817. [CrossRef] [PubMed]
110. Perna, L.; Alongi, F.; Fiorino, C.; Broggi, S.; Cattaneo Giovanni, M.; Cozzarini, C.; Di Muzio, N.; Calandrino, R. Predictors of acute bowel toxicity in patients treated with IMRT whole pelvis irradiation after prostatectomy. *Radiother. Oncol.* **2010**, *97*, 71–75. [CrossRef] [PubMed]
111. Tomita, N.; Soga, N.; Ogura, Y.; Hayashi, N.; Shimizu, H.; Kubota, T.; Ito, J.; Hirata, K.; Ohshima, Y.; Tachibana, H.; et al. Preliminary analysis of risk factors for late rectal toxicity after helical tomotherapy for prostate cancer. *J. Radiat. Res.* **2013**, *54*, 919–924. [CrossRef] [PubMed]
112. Norkus, D.; Karklelyte, A.; Engels, B.; Versmessen, H.; Griskevicius, R.; De Ridder, M.; Storme, G.; Aleknavicius, E.; Janulionis, E.; Valuckas, K.P. A randomized hypofractionation dose escalation trial for high risk prostate cancer patients: Interim analysis of acute toxicity and quality of life in 124 patients. *Radiat. Oncol.* **2013**, *8*, 206. [CrossRef] [PubMed]
113. Viani, G.A.; da Silva, L.B.G.; da Silva, B.B.; Crempe, Y.B.; Martins, V.S.; Ferrari, R.J.R.; Pólo, M.C.; Rossi, B.T.; Suguikawa, E.; Zulliani, G.C.; et al. Acute toxicity profile in prostate cancer with conventional and hypofractionated treatment. *Radiat. Oncol.* **2013**, *8*, 94. [CrossRef]
114. Ippolito, E.; Deodato, F.; Macchia, G.; Massaccesi, M.; Digesù, C.; Pirozzi, G.A.; Spera, G.; Marangi, S.; Annoscia, E.; Cilla, S.; et al. Early radiation-induced mucosal changes evaluated by proctoscopy: Predictive role of dosimetric parameters. *Radiother. Oncol.* **2012**, *104*, 103–108. [CrossRef]
115. Kong, M.; Hong, S.E.; Chang, S.-G. Hypofractionated helical tomotherapy (75 Gy at 2.5 Gy per fraction) for localized prostate cancer: Long-term analysis of gastrointestinal and genitourinary toxicity. *OncoTargets Ther.* **2014**, *7*, 553–566. [CrossRef]
116. Park, J.-H.; Kim, Y.S.; Park, J.; Ahn, H.; Kim, C.-S.; Kim, M.; Kim, J.H.; Ahn, S.D. Incidence and dose-volume analysis of acute bladder toxicity following pelvic radiotherapy. *Tumori* **2014**, *100*, 195–200. [CrossRef]
117. Sini, C.; Fiorino, C.; Perna, L.; Noris Chiorda, B.; Deantoni, C.L.; Bianchi, M.; Sacco, V.; Briganti, A.; Montorsi, F.; Calandrino, R.; et al. Dose-volume effects for pelvic bone marrow in predicting hematological toxicity in prostate cancer radiotherapy with pelvic node irradiation. *Radiother. Oncol.* **2016**, *118*, 79–84. [CrossRef]
118. Cozzarini, C.; Rancati, T.; Carillo, V.; Civardi, F.; Garibaldi, E.; Franco, P.; Avuzzi, B.; Esposti, C.D.; Girelli, G.; Iotti, C.; et al. Multi-variable models predicting specific patient-reported acute urinary symptoms after radiotherapy for prostate cancer: Results of a cohort study. *Radiother. Oncol.* **2015**, *116*, 185–191. [CrossRef]
119. Stankovic, V.; Nikitovic, M.; Pekmezovic, T.; Pekmezovic, D.; Kisic Tepavcevic, D.; Stefanovic Djuric, A.; Saric, M. Toxicity of the lower gastrointestinal tract and its predictive factors after 72Gy conventionally fractionated 3D conformal radiotherapy of localized prostate cancer. *J. BUON* **2016**, *21*, 1224–1232. [PubMed]
120. Bagalà, P.; Ingrosso, G.; Falco, M.D.; Petrichella, S.; D'Andrea, M.; Rago, M.; Lancia, A.; Bruni, C.; Ponti, E.; Santoni, R. Predicting genitourinary toxicity in three-dimensional conformal radiotherapy for localized prostate cancer: A dose-volume parameters analysis of the bladder. *J. Cancer Res. Ther.* **2016**, *12*, 1018–1024. [CrossRef] [PubMed]
121. Son, C.H.; Melotek, J.M.; Liao, C.; Hubert, G.; Pelizzari, C.A.; Eggener, S.E.; Liauw, S.L. Bladder dose-volume parameters are associated with urinary incontinence after postoperative intensity modulated radiation therapy for prostate cancer. *Pract. Radiat. Oncol.* **2016**, *6*, e179–e185. [CrossRef] [PubMed]
122. Arunsingh, M.; Mallick, I.; Prasath, S.; Arun, B.; Sarkar, S.; Shrimali, R.K.; Chatterjee, S.; Achari, R. Acute toxicity and its dosimetric correlates for high-risk prostate cancer treated with moderately hypofractionated radiotherapy. *Med. Dosim.* **2017**, *42*, 18–23. [CrossRef]
123. Katahira-Suzuki, R.; Omura, M.; Takano, S.; Matsui, K.; Hongo, H.; Yamakabe, W.; Nagata, H.; Hashimoto, H.; Miura, I.; Inoue, T. Clinical and dosimetric predictors of late rectal bleeding of prostate cancer after TomoTherapy intensity modulated radiation therapy. *J. Med. Radiat. Sci.* **2017**, *64*, 172–179. [CrossRef]
124. Mostafaei, S.; Abdollahi, H.; Kazempour Dehkordi, S.; Shiri, I.; Razzaghdoust, A.; Zoljalali Moghaddam, S.H.; Saadipoor, A.; Koosha, F.; Cheraghi, S.; Mahdavi, S.R. CT imaging markers to improve radiation toxicity prediction in prostate cancer radiotherapy by stacking regression algorithm. *Radiol. Med.* **2020**, *125*, 87–97. [CrossRef]
125. Peng, X.; Zhou, S.; Liu, S.; Li, J.; Huang, S.; Jiang, X.; Lin, M.; Huang, S.; Lin, C.; Qian, C.; et al. Dose-volume analysis of predictors for acute anal toxicity after radiotherapy in prostate cancer patients. *Radiat. Oncol.* **2019**, *14*, 174. [CrossRef]
126. Catucci, F.; Alitto, A.R.; Masciocchi, C.; Dinapoli, N.; Gatta, R.; Martino, A.; Mazzarella, C.; Fionda, B.; Frascino, V.; Piras, A.; et al. Predicting Radiotherapy Impact on Late Bladder Toxicity in Prostate Cancer Patients: An Observational Study. *Cancers* **2021**, *13*, 175. [CrossRef]
127. Bresolin, A.; Faiella, A.; Garibaldi, E.; Munoz, F.; Cante, D.; Vavassori, V.; Waskiewicz, J.M.; Girelli, G.; Avuzzi, B.; Villa, E.; et al. Acute patient-reported intestinal toxicity in whole pelvis IMRT for prostate cancer: Bowel dose-volume effect quantification in a multicentric cohort study. *Radiother. Oncol.* **2021**, *158*, 74–82. [CrossRef]

128. Ong, A.L.K.; Knight, K.; Panettieri, V.; Dimmock, M.; Tuan, J.K.L.; Tan, H.Q.; Wright, C. Dose-volume analysis of planned versus accumulated dose as a predictor for late gastrointestinal toxicity in men receiving radiotherapy for high-risk prostate cancer. *Phys. Imaging Radiat. Oncol.* **2022**, *23*, 97–102. [CrossRef]
129. Fenlon, J.B.; Nelson, G.; Teague, K.M.; Coleman, S.; Shrieve, D.; Tward, J. A Dosimetric Correlation Between Radiation Dose to Bone and Reduction of Hemoglobin Levels After Radiation Therapy for Prostate Cancer. *Int. J. Radiat. Oncol. Biol. Phys.* **2024**, *118*, 85–93. [CrossRef] [PubMed]
130. Fawcett, T. An introduction to ROC analysis. *Pattern Recognit. Lett.* **2006**, *27*, 861–874. [CrossRef]
131. Christiansen, R.L.; Dysager, L.; Hansen, C.R.; Jensen, H.R.; Schytte, T.; Nyborg, C.J.; Bertelsen, A.S.; Agergaard, S.N.; Mahmood, F.; Hansen, S.; et al. Online adaptive radiotherapy potentially reduces toxicity for high-risk prostate cancer treatment. *Radiother. Oncol.* **2022**, *167*, 165–171. [CrossRef]
132. Green, D.E.; Rubin, C.T. Consequences of irradiation on bone and marrow phenotypes, and its relation to disruption of hematopoietic precursors. *Bone* **2014**, *63*, 87–94. [CrossRef]
133. Arcadipane, F.; Silvetti, P.; Olivero, F.; Gastino, A.; De Luca, V.; Mistrangelo, M.; Cassoni, P.; Racca, P.; Gallio, E.; Lesca, A.; et al. Bone Marrow-Sparing IMRT in Anal Cancer Patients Undergoing Concurrent Chemo-Radiation: Results of the First Phase of a Prospective Phase II Trial. *Cancers* **2020**, *12*, 3306. [CrossRef]
134. Shadad, A.K.; Sullivan, F.J.; Martin, J.D.; Egan, L.J. Gastrointestinal radiation injury: Symptoms, risk factors and mechanisms. *World J. Gastroenterol.* **2013**, *19*, 185–198. [CrossRef]
135. Lapierre, A.; Bourillon, L.; Larroque, M.; Gouveia, T.; Bourgier, C.; Ozsahin, M.; Pèlegrin, A.; Azria, D.; Brengues, M. Improving Patients' Life Quality after Radiotherapy Treatment by Predicting Late Toxicities. *Cancers* **2022**, *14*, 2097. [CrossRef] [PubMed]
136. Bisello, S.; Cilla, S.; Benini, A.; Cardano, R.; Nguyen, N.P.; Deodato, F.; Macchia, G.; Buwenge, M.; Cammelli, S.; Wondemagegnehu, T.; et al. Dose-Volume Constraints fOr oRganS At risk In Radiotherapy (CORSAIR): An "All-in-One" Multicenter-Multidisciplinary Practical Summary. *Curr. Oncol.* **2022**, *29*, 7021–7050. [CrossRef] [PubMed]
137. Choi, H.S.; Jo, G.S.; Chae, J.P.; Lee, S.B.; Kim, C.H.; Jeong, B.K.; Jeong, H.; Lee, Y.H.; Ha, I.B.; Kang, K.M.; et al. Defining the Optimal Time of Adaptive Replanning in Prostate Cancer Patients with Weight Change during Volumetric Arc Radiotherapy: A Dosimetric and Mathematical Analysis Using the Gamma Index. *Comput. Math. Methods Med.* **2017**, *2017*, 4149591. [CrossRef]
138. Marks, L.B.; Yorke, E.D.; Jackson, A.; Ten Haken, R.K.; Constine, L.S.; Eisbruch, A.; Bentzen, S.M.; Nam, J.; Deasy, J.O. The Use of Normal Tissue Complication Probability (NTCP) Models in the Clinic. *Int. J. Radiat. Oncol. Biol. Phys.* **2010**, *76*, S10–S19. [CrossRef]
139. Feuvret, L.; Noël, G.; Mazeron, J.-J.; Bey, P. Conformity index: A review. *Int. J. Radiat. Oncol. Biol. Phys.* **2006**, *64*, 333–342. [CrossRef] [PubMed]
140. Das, S.; Kharade, V.; Pandey, V.; KV, A.; Pasricha, R.K.; Gupta, M. Gamma Index Analysis as a Patient-Specific Quality Assurance Tool for High-Precision Radiotherapy: A Clinical Perspective of Single Institute Experience. *Cureus* **2022**, *14*, e30885. [CrossRef] [PubMed]
141. Liao, J.; Li, X.; Gan, Y.; Han, S.; Rong, P.; Wang, W.; Li, W.; Zhou, L. Artificial intelligence assists precision medicine in cancer treatment. *Front. Oncol.* **2023**, *12*, 998222. [CrossRef] [PubMed]
142. Wei, L.; Niraula, D.; Gates, E.D.H.; Fu, J.; Luo, Y.; Nyflot, M.J.; Bowen, S.R.; El Naqa, I.M.; Cui, S. Artificial intelligence (AI) and machine learning (ML) in precision oncology: A review on enhancing discoverability through multiomics integration. *Br. J. Radiol.* **2023**, *96*, 20230211. [CrossRef] [PubMed]
143. Niraula, D.; Jamaluddin, J.; Matuszak, M.M.; Haken, R.K.T.; Naqa, I.E. Quantum deep reinforcement learning for clinical decision support in oncology: Application to adaptive radiotherapy. *Sci. Rep.* **2021**, *11*, 23545. [CrossRef]
144. Luo, Y.; Tseng, H.-H.; Cui, S.; Wei, L.; Ten Haken, R.K.; El Naqa, I. Balancing accuracy and interpretability of machine learning approaches for radiation treatment outcomes modeling. *BJR Open* **2019**, *1*, 20190021. [CrossRef]
145. Kearney, M.; Coffey, M.; Rossi, M.; Tsang, Y. ESTRO ROSQC, RTTC Future-proof Radiation therapist (RTT) practice in a pandemic-Lessons learnt from COVID-19. *Tech. Innov. Patient Support. Radiat. Oncol.* **2021**, *17*, 18–24. [CrossRef]
146. Lee, S.; Kerns, S.; Ostrer, H.; Rosenstein, B.; Deasy, J.O.; Oh, J.H. Machine Learning on a Genome-wide Association Study to Predict Late Genitourinary Toxicity After Prostate Radiation Therapy. *Int. J. Radiat. Oncol. Biol. Phys.* **2018**, *101*, 128. [CrossRef]
147. Abdollahi, H.; Tanha, K.; Mofid, B.; Razzaghdoust, A.; Saadipoor, A.; Khalafi, L.; Bakhshandeh, M.; Mahdavi, S.R. MRI Radiomic Analysis of IMRT-Induced Bladder Wall Changes in Prostate Cancer Patients: A Relationship with Radiation Dose and Toxicity. *J. Med. Imaging Radiat. Sci.* **2019**, *50*, 252–260. [CrossRef]
148. Carrara, M.; Massari, E.; Cicchetti, A.; Giandini, T.; Avuzzi, B.; Palorini, F.; Stucchi, C.; Fellin, G.; Gabriele, P.; Vavassori, V.; et al. Development of a Ready-to-Use Graphical Tool Based on Artificial Neural Network Classification: Application for the Prediction of Late Fecal Incontinence After Prostate Cancer Radiation Therapy. *Int. J. Radiat. Oncol. Biol. Phys.* **2018**, *102*, 1533–1542. [CrossRef]
149. Moulton, C.R.; House, M.J.; Lye, V.; Tang, C.I.; Krawiec, M.; Joseph, D.J.; Denham, J.W.; Ebert, M.A. Spatial features of dose-surface maps from deformably-registered plans correlate with late gastrointestinal complications. *Phys. Med. Biol.* **2017**, *62*, 4118–4139. [CrossRef] [PubMed]
150. Fargeas, A.; Albera, L.; Kachenoura, A.; Dréan, G.; Ospina, J.-D.; Coloigner, J.; Lafond, C.; Delobel, J.-B.; De Crevoisier, R.; Acosta, O. On feature extraction and classification in prostate cancer radiotherapy using tensor decompositions. *Med. Eng. Phys.* **2015**, *37*, 126–131. [CrossRef] [PubMed]

151. Abdollahi, H.; Mahdavi, S.R.; Mofid, B.; Bakhshandeh, M.; Razzaghdoust, A.; Saadipoor, A.; Tanha, K. Rectal wall MRI radiomics in prostate cancer patients: Prediction of and correlation with early rectal toxicity. *Int. J. Radiat. Biol.* **2018**, *94*, 829–837. [CrossRef] [PubMed]
152. Pan, X.; Levin-Epstein, R.; Huang, J.; Ruan, D.; King, C.R.; Kishan, A.U.; Steinberg, M.L.; Qi, X.S. Dosimetric predictors of patient-reported toxicity after prostate stereotactic body radiotherapy: Analysis of full range of the dose–volume histogram using ensemble machine learning. *Radiother. Oncol.* **2020**, *148*, 181–188. [CrossRef]
153. Saito, T.; Rehmsmeier, M. The Precision-Recall Plot Is More Informative than the ROC Plot When Evaluating Binary Classifiers on Imbalanced Datasets. *PLoS ONE* **2015**, *10*, e0118432. [CrossRef]
154. Zhao, W.; Shen, L.; Islam, M.T.; Qin, W.; Zhang, Z.; Liang, X.; Zhang, G.; Xu, S.; Li, X. Artificial intelligence in image-guided radiotherapy: A review of treatment target localization. *Quant. Imaging Med. Surg.* **2021**, *11*, 4881–4894. [CrossRef]
155. Corradini, D.; Brizi, L.; Gaudiano, C.; Bianchi, L.; Marcelli, E.; Golfieri, R.; Schiavina, R.; Testa, C.; Remondini, D. Challenges in the Use of Artificial Intelligence for Prostate Cancer Diagnosis from Multiparametric Imaging Data. *Cancers* **2021**, *13*, 3944. [CrossRef]
156. Fiagbedzi, E.; Hasford, F.; Tagoe, S.N. The influence of artificial intelligence on the work of the medical physicist in radiotherapy practice: A short review. *BJR Open* **2023**, *5*, 20230003. [CrossRef]
157. Liu, J.; Xiao, H.; Fan, J.; Hu, W.; Yang, Y.; Dong, P.; Xing, L.; Cai, J. An overview of artificial intelligence in medical physics and radiation oncology. *J. Natl. Cancer Cent.* **2023**, *3*, 211–221. [CrossRef]
158. Alowais, S.A.; Alghamdi, S.S.; Alsuhebany, N.; Alqahtani, T.; Alshaya, A.I.; Almohareb, S.N.; Aldairem, A.; Alrashed, M.; Bin Saleh, K.; Badreldin, H.A.; et al. Revolutionizing healthcare: The role of artificial intelligence in clinical practice. *BMC Med. Educ.* **2023**, *23*, 689. [CrossRef]
159. Cui, S.; Traverso, A.; Niraula, D.; Zou, J.; Luo, Y.; Owen, D.; El Naqa, I.; Wei, L. Interpretable artificial intelligence in radiology and radiation oncology. *Br. J. Radiol.* **2023**, *96*, 20230142. [CrossRef] [PubMed]
160. Hurvitz, N.; Ilan, Y. The Constrained-Disorder Principle Assists in Overcoming Significant Challenges in Digital Health: Moving from "Nice to Have" to Mandatory Systems. *Clin. Pract.* **2023**, *13*, 994–1014. [CrossRef] [PubMed]
161. Singh, Y.; Hathaway, Q.A.; Erickson, B.J. Generative AI in oncological imaging: Revolutionizing cancer detection and diagnosis. *Oncotarget* **2024**, *15*, 607–608. [CrossRef] [PubMed]
162. Vallée, A. Envisioning the Future of Personalized Medicine: Role and Realities of Digital Twins. *J. Med. Internet Res.* **2024**, *26*, e50204. [CrossRef] [PubMed]
163. Wang, Y.; Fu, T.; Xu, Y.; Ma, Z.; Xu, H.; Lu, Y.; Du, B.; Gao, H.; Wu, J. TWIN-GPT: Digital Twins for Clinical Trials via Large Language Model 2024. In *ACM Transactions on Multimedia Computing, Communications and Applications*; ACM, Inc.: New York, NY, USA, 2024. [CrossRef]
164. Jones, S.; Thompson, K.; Porter, B.; Shepherd, M.; Sapkaroski, D.; Grimshaw, A.; Hargrave, C. Automation and artificial intelligence in radiation therapy treatment planning. *J. Med. Radiat. Sci.* **2024**, *71*, 290–298. [CrossRef]
165. Panettieri, V.; Gagliardi, G. Artificial Intelligence and the future of radiotherapy planning: The Australian radiation therapists prepare to be ready. *J. Med. Radiat. Sci.* **2024**, *71*, 174–176. [CrossRef]
166. Kalsi, S.; French, H.; Chhaya, S.; Madani, H.; Mir, R.; Anosova, A.; Dubash, S. The Evolving Role of Artificial Intelligence in Radiotherapy Treatment Planning—A Literature Review. *Clin. Oncol.* **2024**, *36*, 596–605. [CrossRef]
167. Gerke, S.; Minssen, T.; Cohen, G. Ethical and legal challenges of artificial intelligence-driven healthcare. In *Artificial Intelligence in Healthcare*; Academic Press: New York, NY, USA, 2020; pp. 295–336. [CrossRef]
168. Jeyaraman, M.; Balaji, S.; Jeyaraman, N.; Yadav, S. Unraveling the Ethical Enigma: Artificial Intelligence in Healthcare. *Cureus* **2023**, *15*, e43262. [CrossRef]